GEOTHERMAL TRAINING PROGRAMME
Orkustofnun, Grensásvegur 9,
IS-108 Reykjavík, Iceland

Reports 2000
Number 7

STUDY ON DEEP GEOTHERMAL DRILLING INTO A SUPERCRITICAL ZONE IN ICELAND

Huang Hefu
Dian Qian Gui Drilling Company, SINOPEC,
LinYi County,
Shandong Province, 251500,
P.R. CHINA
huanghefu@sina.com

ABSTRACT

Practical and environmental reasons will call for increasingly deeper drilling for exploiting high-temperature geothermal fields in the 21st century. The Icelandic geothermal community is planning a joint deep geothermal drilling research project, ICELAND DEEP DRILLING PROJECT (IDDP), on the Reykjanes peninsula - the landward extension of the Reykjanes Ridge. The principal aim is to bring supercritical hydrous fluid (400-600°C) up to the surface under high pressure, through a 4-5 km deep drillhole, into a research pilot plant where the thermal energy of the fluid is used and the chemicals extracted. When drilling into supercritical conditions, many problems may occur due to severe conditions related to increasing well depth and rising temperatures and pressures, so new advanced technology is needed. If successful, the technical gain from deep drilling and research could have a global impact on future geothermal utilization.

1. INTRODUCTION

With the requirement of increasing fluid production rates and higher wellhead pressures, the target depth of geothermal energy development has increased in many countries. Several 3000-4000 m deep geothermal wells have been drilled in Italy, the USA and Mexico, Japan, New Zealand and the Philippines. In some wells the formation temperature exceeds 350°C and in well WD-1A in Kakonda, Japan, temperatures greater than 500°C were encountered. In Iceland, the country most developed with regards geothermal energy, the deepest high-temperature well is 2500 m deep and the deepest low-temperature well is 3030 m. The Icelandic geothermal community is planning to join in a deep geothermal drilling research project on the Reykjanes Peninsula - the landward extension of the Reykjanes Ridge. The purpose is to bring supercritical hydrous fluid (400-600°C) up to the surface under high pressure, through a 4–5 km deep drillhole, into a research pilot plant (Fridleifsson and Albertsson, 2000). Drilling such a geothermal well is a challenging project on an international scale.

Supercritical conditions are reached when temperature is greater than 374°C and the pressure above 220 bars, the critical point. When a hole is drilled into supercritical conditions, the bottom hole temperatures may reach 400-600°C. There are reports of bottom hole temperature greater than 374°C. One case was in Iceland, in well NJ-11 at Nesjavellir where the measured bottom hole temperatures was 380°C. Another case was reported in Hawaii; the well produced steam/fluid at surface at 374°C. Both wells were not thought to be deep enough to reach supercritical conditions, but possibly intersected a fracture connected to the supercritical fluid. A third case was reported in Japan, well WD-1A in Kakonda, where the formation temperature exceeded 500°C at 3700 m depth; this was one of the HDR (hot dry rock) wells. With increasing bottom hole temperatures, many downhole problems will occur. Cyclic steam stimulation can impose severe stresses on the casing. If the temperature is high enough, the yield strength of the casing materials will be exceeded and the casing will become plastically deformed or collapse, leading to early casing damage. The high temperature and pressure can also lead to blowouts. Many downhole tools and materials also have temperature limitations. How to estimate the bottom hole temperature and cool the well while drilling is important for successful drilling. This paper will assess some of the problems to be encountered while drilling a well into the supercritical zone. How these critical problems are dealt with is a key issue for success of high-temperature well drilling.

2. DRILLSITE SELECTION AND GEOLOGICAL CONDITIONS

2.1 Drillsite selection

Iceland is located in the Mid-Atlantic Ridge region. The boundary between the European and American plates is along the axial rift zone running across Iceland. It is characterized by many volcanic systems arranged en-echelon along the rift zone. Like other constructive plates margins the Mid-Atlantic Ridge is characterized by high heat flow in the crustal region, but with increasing distance symmetrically away from the ridge crest, the mean heat flow falls until it reaches an average level of the oceans. Iceland forms a 500 km broad segment astride the ridge and falls entirely within the crustal heat flow anomaly. The regional heat flow on the island varies from about 80 mW/m^2 furthest away from the active volcanic zone crossing the country to about 300 mW/m^2 in some regions at the margins of the Reykjanes-Langjökull axial rift zone (Figure 1).

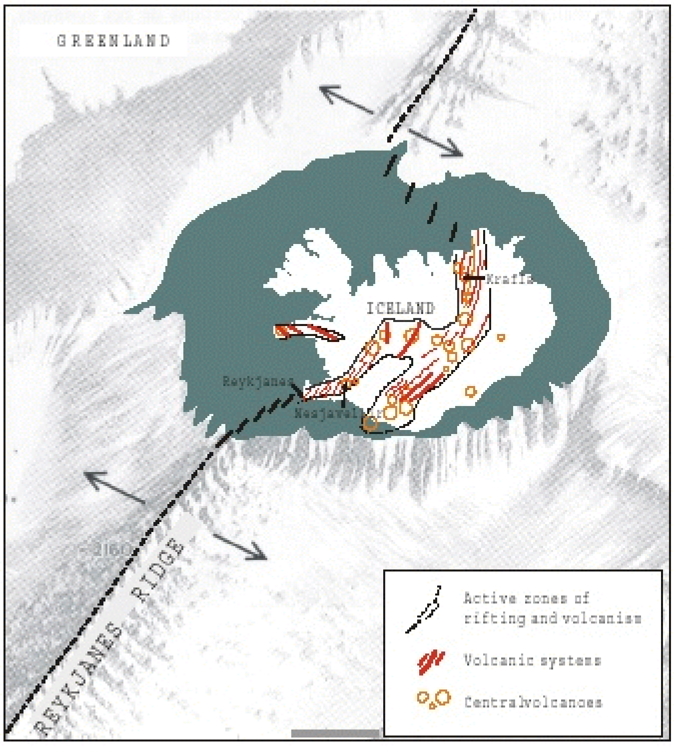

FIGURE 1: Iceland and the Mid-Atlantic Ridge; locations of Reykjanes, Nesjavellir and Krafla high-temperature fields are shown (Fridleifsson and Albertsson, 2000)

Hot springs are very abundant in the country as the result of the high heat flow. To date, approximately 1000 geothermal localities in the country have been recognized. For the IDDP, only the better studied high-temperature systems, i.e. the Krafla-, Nesjavellir-, Svartsengi-, and the Reykjanes geothermal systems are targeted. All four are already utilised, producing electricity with steam and/or producing hot water for domestic use through heat exchangers. Of these four systems, the Svartsengi system will not be discussed further, as it is probably the least suitable for deep research drilling for supercritical fluids. The Reykjanes system on the other hand, is much hotter and exploited on a limited scale at present, where high-quality salts are extracted from the high-temperature geothermal brine. Partly for these reasons the Reykjanes system is the main candidate for the joint research programme (IDDP), financed by the main energy producers in Iceland, possibly with participation of an international consortium of researchers and equipment manufactures. This IDDP project was introduced at the World Geothermal Congress 2000 in Japan (Fridleifsson and Albertsson, 2000).

Reykjanes can be considered a natural drilling platform above a mid-ocean-ridge high-temperature system. Its seawater salinity, its high metal content and its open fracture system on the spreading Reykjanes ridge, seem to be an ideal setting for pilot plant studies on high pressure-temperature to harness similar fluids as thrive within the black smokers on ocean ridges. Nevertheless, in selecting a suitable drillsite for research on supercritical fluids in Iceland, several options will and need to be discussed by research groups. As yet, the advisory structure for this project has not been established. Tentatively, a drillsite has been selected in a saline hydrothermal system at the tip of the Reykjanes peninsula, the landward extension of the mid-Atlantic ridge (Figure 1). The site selection is made in order to mimic conditions of the ocean floor "black smokers" which are natural geothermal systems at supercritical conditions (Fridleifsson and Albertsson, 2000).

The selected drillsites at Reykjanes flank the surface geothermal manifestations, but are located within the high-temperature system at depth. Supercritical condition may be expected there at drillsites located between a 2000 years old volcanic fissure and a volcanic fissure from historic times (1226 AD). While uncertainty exists on the supercritical conditions at Reykjanes above 4 km depth, a supporting analogue is sought for the time-temperature constraint of a 2000 years old volcanic fissure at Nesjavellir, where a supercritical hydrous fluid was met at 2265 m depth in well NJ-11.

2.2 Geological conditions of the upper part of the Reykjanes hydrothermal field

The Reykjanes high-temperature area is one of many in Iceland, all of which are within the active volcanic belt. Underground temperatures are above 200°C at depths of a few hundred metres. To date, 10 wells have been drilled in the Reykjanes area. Well RN-10 is the deepest drillhole, reaching 2046 m. It penetrates a several hundred meter thick succession of shallow-marine sediments, submarine tuffs and pillow lava formations interbedded with subaerial lava formations in the upper 1 km, and a hyaloclastite formation in between thick lava sequences in the lower 2 km. A total circulation loss of >60 l/s in well RN-10 was met at 1900-2000 m depth in a wollastonite bearing vein system. The formation temperature, judging from the secondary alteration and temperature logs, is well over 300°C.

2.3 Crustal structure and the lower part of the hydrothermal system

Studies of explosion seismology show a low-velocity layer (P-velocity about 3.0 km/s) reaching a depth of 900 m. This low-velocity layer is found everywhere at the surface in the active volcanic belt (Pálmason, 1971) and is considered to correspond to porous and rather fresh volcanic breccias, pillow lavas, and individual lavas flows with a low degree of compaction (density 2.1-2.5 g/cm^3). This has been verified by exploratory drilling. Cores of intensely altered hyaloclastite from 300 and 570 m depths had a porosity of 32% and 23%, respectively.

Below the surface layer to a depth of 2600 m the P-velocity is 4.2 km/s, which is similar to that of Tertiary flood basalts in Iceland. The average density of this layer is 2.6 g/cm^3. An exploratory drillhole reaching 1750 m depth indicates that this formation is built up mainly of basaltic flows with thick interbeds of hyaloclastites. A core of hyaloclastite at 1370 m had a porosity of 19%. No cores were obtained from the basalt lavas, but in that type of formation an average porosity of 3-5% can be expected.

The third seismic layer under the Reykjanes Peninsula has a P-velocity of 6.5 km/s and an average

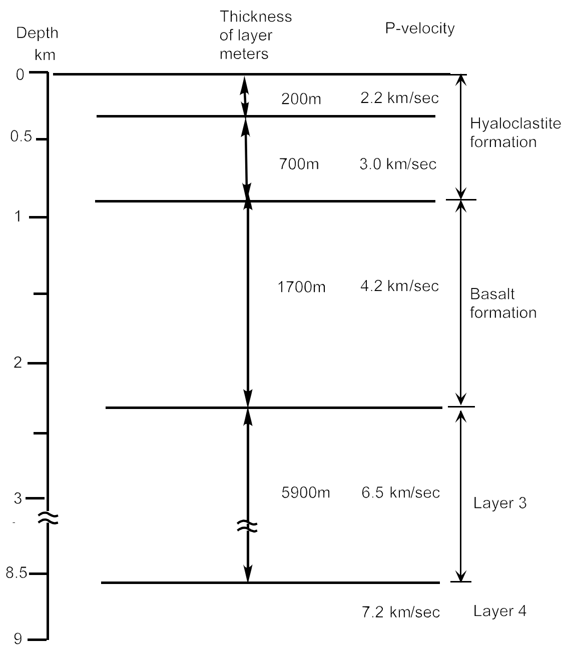

FIGURE 2: Seismic layers in the Reykjanes thermal area (Björnsson et al., 1972)

density of 2.9 g/cm^3. It is underlain at 8.5 km depth by layer 4 which has a P-velocity of 7.2 km/s and an average density of 3.1 g/cm^3 (Pálmason 1971). Layer 3 is considered to correspond to the "oceanic layer" generally found on the floor of the oceans, and layer 4 to the anomalous upper mantle as observed under the critical zone of the mid-ocean ridges (Figure 2).

Temperature gradients in shallow drillhole in southwest Iceland suggest that the upper boundary of layer 3 in this region may have a temperature of 350-400°C (Pálmason, 1971). This would imply that, under the Reykjanes thermal area, the 350°C isotherm is to be found at about 2600 m depth. The nature of the 2-3 layer boundary is not known, but the combined seismic and temperature data suggest that it is a boundary between metamorphic facies of basaltic rocks, perhaps a greenschist-amphibolite boundary. The density and high degree of alteration expected in layer 3 suggest a low permeability in this layer, and whether groundwater can circulate below the boundary between layers 2 and 3 is questionable, despite the low viscosity of water which would be close to critical temperature and pressure (Björnsson, et al., 1972).

3. CRITICAL PROBLEMS OF DEEP DRILLING

3.1 Drillhole temperature and pressure

Basically, the temperatures and pressures in high-temperature geothermal wells in Iceland can be expected to follow the boiling point with depth curve (BPD) based on the assumption of water at boiling conditions at any depth, as is the case at Reykjanes. The highest steam/water temperature which can occur at any chosen depth in a well drilled into such conditions is limited by the governing pressure. For a 4000-5000 m deep exploration well, the bottom hole temperature may exceed 500°C. In such a situation, the bottom hole fluids will be at supercritical conditions. In other places the temperature and pressure may not follow the boiling point curve.

3.1.1 Supercritical conditions

Supercritical conditions are expected in geothermal systems that penetrate deep into the crust where the static pressure exceeds the critical pressure, and where young igneous intrusions can generate supercritical temperatures. On land, these conditions could be found below 3.5 km depth in the crust, assuming boiling conditions in the hydrostatic fluid above. On the sea floor, the hydrostatic head of the ocean may exceed the critical pressure and supercritical temperatures can, therefore, exist at shallow depth beneath the sea floor. However, if there is a vadose zone, or a steam deposit above the hydrothermal zone, then the pressure at the bottom of this sub-hydrostatic zone will be much lower. Therefore, in the permeable, hydrostatic regime, the curve will start there and the supercritical zone will be much deeper than the usual curve indicates. The presence of dissolved salts in geothermal fluids has an important effect on phase transitions. The temperature and pressure of the critical point increase with the increased salinity displacing the conditions for supercritical fluid to greater depth. The boiling temperature of saline water at given pressure is also higher than that of pure water. The effect delays the initiation of boiling in an ascending saline fluid.

The critical point (CP) of supercritical condition for pure water is at 221.2 bar and 374.15°C. If a natural hydrostatic hydrothermal system was at boiling point from the surface down to the critical point, maximum pressure and temperature at each depth would be determined by the boiling point depth curve (BPD-curve), and the CP-point would be reached at about 3.5 km depth. Below that depth the hydrous fluid would be at supercritical conditions, a hydrous gas, and there would be no phase change in the fluid upon further temperature increase at constant or rising pressure. While the hydrostatic BPD-curve controls the maximum pressure-temperature in most hydrothermal systems, temporal exceptions thrive within the systems, because the boiling water column has much lower density than a cold water column. The CP-pressure in a cold water column would, thus, be reached at about 2.3 km depth, instead of 3.5 km in a water column at boiling point.

3.1.2 Temperature, pressure and density of steam/fluids in geothermal systems

Change in liquid density due to temperature changes. Figures 3 and 4 show the density of the water for different temperatures and pressures, also above the critical point. An important characteristic of the "liquid" under discussion is its density. When temperatures and pressures are below 300°C and 100 bar-a, the density of the "liquid" is not very sensitive to temperature change, but with an increase in temperature and pressure from 310°C, 100 bar-a to near the supercritical point (374°C and 220 bar-a), the density of the "liquid" changes rapidly. This means that there are other "inflection points" around the area. For example, under 180 bar-a, temperature increases only a few degrees from 355 to 360°C. The density of the "liquid" decreases from 558.05 kg/m³ to 123.39 kg/m³ (Table 1). Above the supercritical point, density changes softly with a change in temperature.

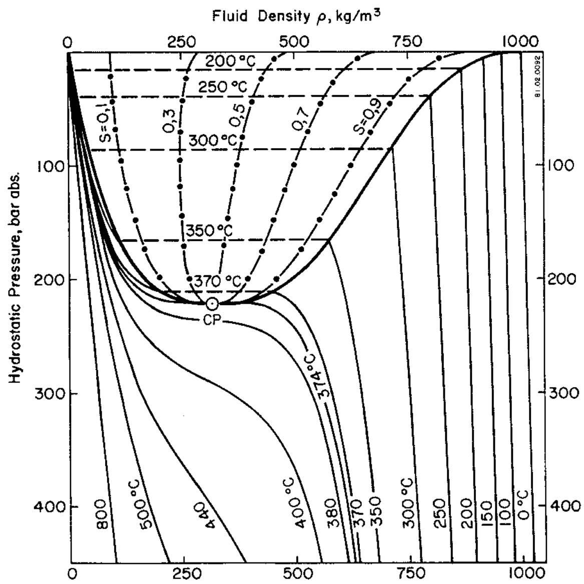

FIGURE 3: Pressure-density diagram for pure water and vapour. Additional parameters are the temperature and water saturation S, based on tables presented by Schmidt (1979); CP: critical point, S: Volume fraction of liquid in fluid (Stefánsson and Björnsson, 1982)

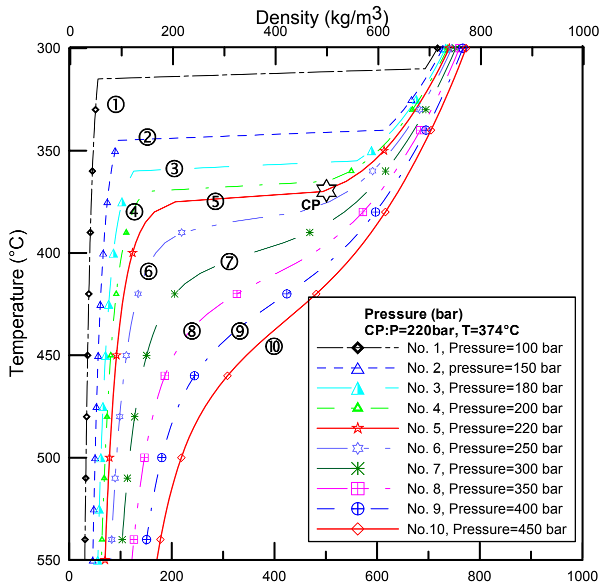

FIGURE 4: Temperature-density diagram for pure water and vapour under different pressures, calculated with the "Steam" program (Bjarnason, 1985)

TABLE 1: Fluid density (kg/m^3) at different temperatures and pressures (steam tables calculated by the STEAM-program; Bjarnason, 1985)

Temp. (°C)	100 (bar-a)	150 (bar-a)	180 (bar-a)	200 (bar-a)	220 (bar-a)	250 (bar-a)	300 (bar-a)	350 (bar-a)	400 (bar-a)	450 (bar-a)
300	715.38	725.74	731.39	734.97	738.4	743.33	751	758.1	764.69	770.89
305	703.6	714.99	721.14	725.01	728.72	734	742.2	749.7	756.68	763.19
310	**690.98**	703.63	710.37	714.58	718.59	724.29	733	741	748.42	755.29
315	**53.74**	691.54	698.98	703.6	707.97	714.14	723.6	732.1	739.92	747.16
320	51.93	678.59	686.9	691.99	696.79	703.51	713.7	722.8	731.14	738.8
335	47.71	632.18	644.9	652.27	658.98	668.07	681.3	692.8	702.94	712.11
340	46.58	**612.6**	628.12	636.77	644.49	654.76	669.4	681.9	692.82	702.61
345	45.55	**92.61**	609.13	619.62	628.69	640.47	656.8	670.5	682.29	692.77
350	44.6	87.24	586.7	600.1	611.16	624.98	643.5	658.6	671.36	682.58
355	43.72	83.05	**558.05**	577.05	591.27	608.01	629.3	646.1	660.02	672.1
360	42.91	79.6	**123.39**	547.38	567.58	588.9	614.1	633	648.31	661.38
365	42.15	76.69	113.1	**501.1**	537.39	566.73	597.4	619	636.01	650.25
370	41.43	74.18	106.05	**144.76**	**491.97**	539.91	578.9	603.9	623	638.6
375	40.76	71.97	100.56	130.47	**204.67**	504.46	558	587.7	609.23	626.41
380	40.12	70.02	96.11	121.27	163.65	446.37	533.7	570	594.61	613.65
400	37.87	63.85	83.94	100.53	121.2	166.28	353.3	473.8	523.8	555.15
425	35.55	58.35	74.7	87.17	101.3	126.81	188.3	292.4	392.41	456.62
450	33.62	54.2	68.33	78.7	89.99	109.04	148.5	201.8	272.12	343.24
475	31.97	50.86	63.48	72.53	82.17	97.89	128.3	165.3	210.3	262.89
500	30.53	48.09	59.58	67.7	76.23	89.86	115.2	144.4	178.08	216.22
525	29.24	45.72	56.33	63.75	71.47	83.65	105.7	130.3	157.66	187.91
550	28.09	43.65	53.56	60.43	67.52	78.61	98.37	119.9	143.24	168.51

Physical states in hydrothermal systems. For discussion, we divide the geothermal system into four regions (Figure 5):

a. Vapour saturation region (1), where the density is less than the density of saturated steam (ρ_{vs}) and the pressure is equal to or less than the critical pressure (P_{crit});
b. Boiling region (2), where two phases are present. The region is enveloped by the Clapeyron curves for saturated vapour (ρ_{vs}) and saturated liquid (ρ_{ls}) at subcritical temperatures and pressures;
c. Liquid saturated region (3), where the temperature is less than the critical temperature (T_{crit}) and the density is greater than the density of saturated liquid (ρ_{ls}) for all $P=P_{crit}$ and greater than ρ (T_{crit},p) for all $P>P_{crit}$;
d. Supercritical region (4), where both temperature and pressure exceed the critical point values ($T_{crit.}$ P_{crit}).

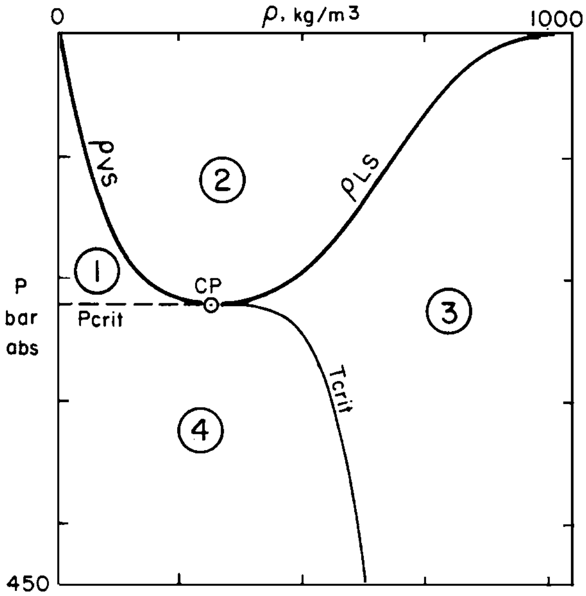

FIGURE 5: Physical states in hydrothermal systems (Stefánsson, and Björnsson, 1982)

Of the four regions, the most important region for discussion of a geothermal system is the two-phase boiling region enveloped by the Clapeyron curves at sub-critical temperatures and pressures (region 2). To uniquely define physical conditions within this region an additional parameter such as water saturation

S, i.e. the volume fraction of water in the fluid, is needed. In the three single-phase regions, the vertical pressure gradient $dp/dz = \rho g$ is proportional to the density ρ of the fluid. In the two-phase region, the density is a weighted average of both phases, assuming that both are present in a homogenous mixture.

Whether this is valid for any geothermal system under undisturbed natural conditions is not obvious. One would observe a vertical pressure gradient intermediate between that for static saturated steam and water, respectively. The intermediate gradient would enhance a counter-current flow of steam and water and aid gravity segregation of the phases. As mentioned above, Martin et al. (1976) found that a given rate of heat flow of two stable conditions of counter-current two-phase flow was theoretically possible, one with high water saturation and liquid dominating the pressure gradient, the other with low water saturation and vapour dominating (Stefánsson and Björnsson, 1982).

3.2 Estimation of formation pressure

Little published information is available describing supercritical drilling operations. Actually, it is not known how high the pressures and temperatures of the formations may go. When drilling into the supercritical zone, the following cases may occur.

Case A: Assume that below the critical point, there is no reservoir to 5000 m, just hot dry rock (HDR). This is a case like that found in well WD-1A drilled in Kakkonda geothermal field in Japan. The well was drilled to 3729 m total depth. According to the borehole temperature data, the formation temperature, without the cooling effects of the drilling operation, could be delineated as follows: 200°C at 300 m depth; 300°C at 1500 m; 400°C at 3200 m; and over 500°C after 159 hours recovery time below 3500 m (Saito and Sakuma, 1997). The bottom hole pressures follow the water column pressure. In such a case, there is not very much impact on drilling and completion of the well (Figure 6).

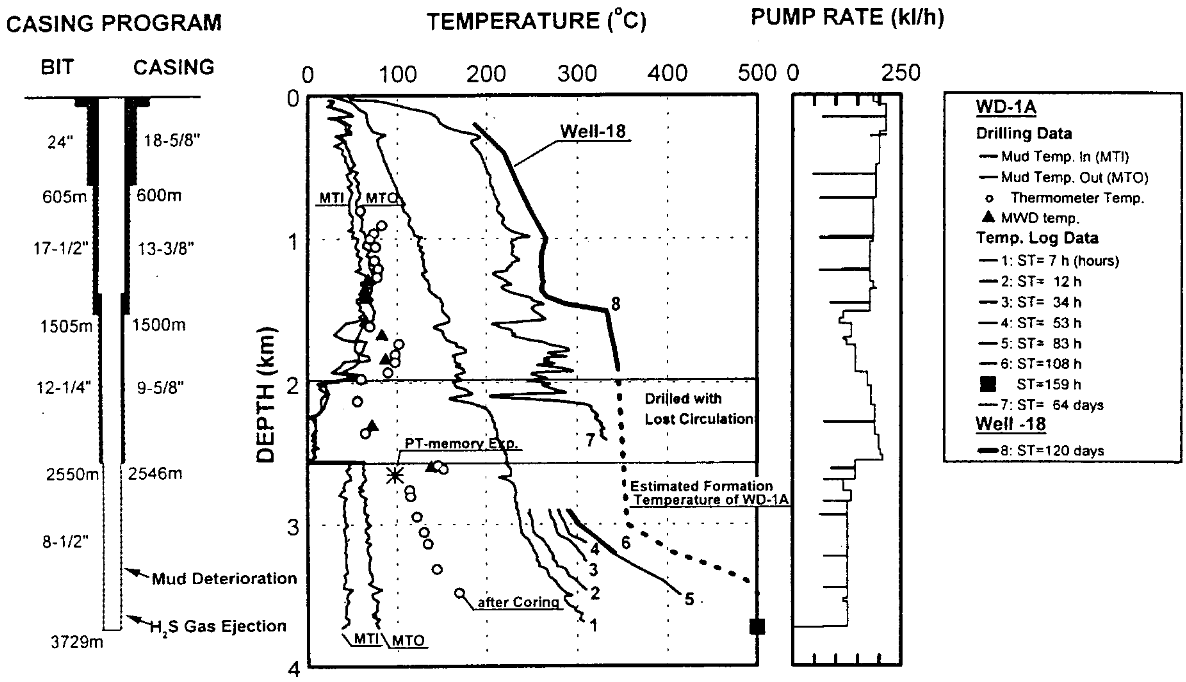

FIGURE 6: WD-1A dynamic borehole temperature data. MTI, MTO: Drilling fluid temperature measured at suction line and flow line. Thermometer temperature was measured with thermometers insider BHA about 15 m above the bit, recorded less than 1.5 hours after circulation ceased. MWD temperature: bottom hole circulation temperature measured with MWD tools; black square shows temperature measured by melting temperature of thermal indication material; ST: recovery time since circulation stopped. Temperature logs 1 through 4 and 7 were recorded with platinum resistance thermometers; temperature logs 5, 6 and 8 were recorded with a Kuster temperature instrument (Saito and Sakuma, 1997)

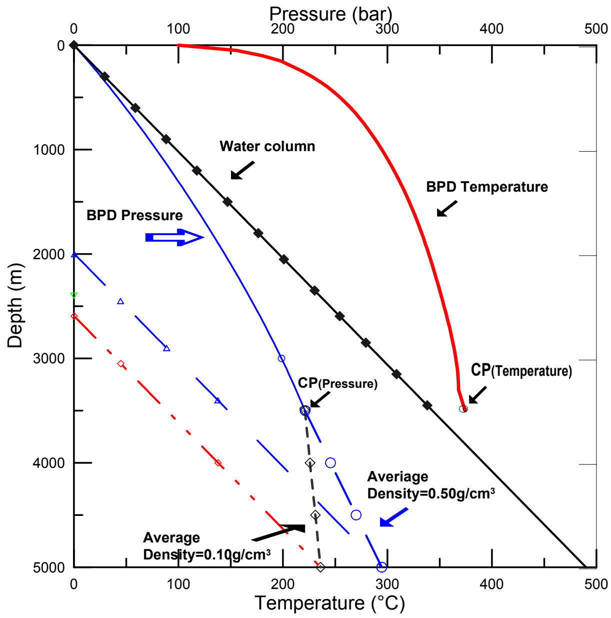

FIGURE 7: Estimated bottom hole pressures

Case B: Assume there is a reservoir somewhere below the critical point. Actually we do not know how high the pressures and temperatures may go in such a reservoir. According to the BPD curve, at Critical Point (about 3500 m depth), the equivalence density of the "liquid" is about 0.65 g/cm^3. Actually, the "liquid" density is about 0.50 g/cm^3 at that depth, and when temperature increases a few degrees, the density decreases very rapidly. For this study, it is assumed that the maximum density of the "liquid" at supercritical conditions is 0.50 g/cm^3. With an increase of the formation temperature, the density of the "liquid" will decrease. It is assumed that the minimum density of the "supercritical liquid" is 0.10 g/cm^3. Estimation of the maximum pressures and the minimum pressures of the reservoir in the supercritical zone can thus be made (Figure 7). In the latter case, there will be some problems for drilling. Should there be a big loss of circulation in the reservoir, the water level could drop down to about 2600 m depth! When drilling into these conditions, if we do not have enough water to fill the well, the well would be heated up very quickly due to inflow of water, that could lead to an underground blowout if the last casing string does not seal off the weak zones above.

Case C: Assume the reservoir to be fracture-dominated, intersecting a fracture network connected to the deeper supercritical zone. One example of this is the well drilled on the Big Island of Hawaii, the first deep geothermal well drilled on Hawaii. The well was drilled some time ago, and it was reported to produce steam/fluids at the surface at 374°C. It was not thought to be deep enough to produce from the supercritical zone. However, it was producing steam/fluids from fractures in volcanic rocks, and it seems possible that this fracture network could have intersected a deeper zone that was at supercritical conditions.

Another example is well NJ-11 drilled in 1985 in the Nesjavellir high-temperature geothermal field in Iceland. The well was drilled to 2265 m total depth, a 13⅜" anchor casing was cemented down to 183 m and a 9⅝" casing to 556 m depth. A total circulation loss occurred at 115 m depth. This warm ground water aquifer has a static water table at 70 m depth and is sealed behind the anchor casing. Two feed zones connected to the shallow geothermal aquifer were intersected at 414 and 518 m depth. The feed zones were over-pressurized compared to the cold circulating water column. There was about 5-6 bar-g overpressure at the wellhead when circulation was stopped, and during drilling a circulation gain of some 35 l/s was measured. The estimated temperatures of the two feed zones were 220 and 245°C, respectively. The production part of the well was drilled with an 8½" bit. Feed zones connected to shallow aquifers were intersected in the depth interval 600-900 m. A wellhead pressure of 2.5 bar-g was measured and when circulation was stopped the immediate flow from the well was 6 l/s. Circulation loss was measured when the well was about 1130 m deep, and at 1226 m total loss occurred (>40 l/s). Drilling continued to 2265 m total depth with a variable loss of 10-40 l/s. A temperature survey was run in the well during one of the circulation stops, see Figure 8. The upper part of the temperature logs was measured with a thermo-electric tool while 44 l/s of cold water were being pumped down the annulus at 6.8 bar-g wellhead pressure. Due to high temperatures the logging was stopped just above 1200 m depth and the deeper parts of the well had to be logged with a mechanical Amerada gauge. Temperature readings were taken at four levels in the well. At 1300 and 1600 m depth the measured temperature was 324 and 333°C, respectively, but at 1900 and 2000 m depth the gauge showed full deflection, indicating the temperatures at these depths exceeded 381°C, the full deflection temperature limit of the tool used. The temperature log in Figure 8 shows counter-flow in the well. The water injected at the wellhead flows down the well, some of it probably lost into the feed zones at 650-900 m depth, but most of it reaches the feed zone at 1226 m where it meets an up-flow originating in the bottom region of the well. The inflow temperature of the deep aquifer is at least 380°C, but the temperature in the up-flow drops due to additional inflow between 1600 and 1900 m depth and boiling above 1600 m. This was a typical case of an underground blowout. The well was not drilled deep enough to reach the supercritical zone, but the temperature was higher than the supercritical temperature. It seems possible that the well intersected a fracture connected to the deeper supercritical zone. When drilling into such a zone, the energic nature of such fluids could be moderated because there was a pressure drop between the deeper fluids and the surface. This case is a very dangerous case because it may lead to a terrible blowout.

Case D: A self-sealed zone below the critical point. Given that magmatic fluid tends to accumulate in plastic rock at lithostatic pressure, and that fluids at hydrostatic pressure circulate through brittle rock where permeability is maintained by recurrent seismic activity, the nature of the interface between these two different hydrologic regimes is of considerable theoretical interest and practical importance in the development of models for ore deposition. In the brittle regime, when dilute solutions in contact with quartz at hydrostatic pressure are slowly heated up at pressures ranging from about 34 to 900 bar (maintaining saturation with respect to the solubility of quartz), a point is reached at which there is a change from dissolution of quartz to precipitation of quartz with further heating (retrograde solubility). Figure 9 shows the calculated solubilities of quartz as a function of temperature at selected isobars. It also shows the region of retrograde solubility where precipitation occurs upon heating at constant P_f (shaded area). Where the circulation of a relatively dilute fluid at hydrostatic pressure extends downward to near the top of a cooling pluton, at a depth of about 3-4 km (300-400 bars, Figure 9), the onset of quartz deposition with heating would occur at about 370-390°C. Increasing salinity and pressure (at greater depths of circulation) move the point of maximum quartz solubility to >400°C (Figure 10). However, at >400°C quartz diorite starts to become quasiplastic and this limits the time that fractures are likely to remain open for fluid flow.

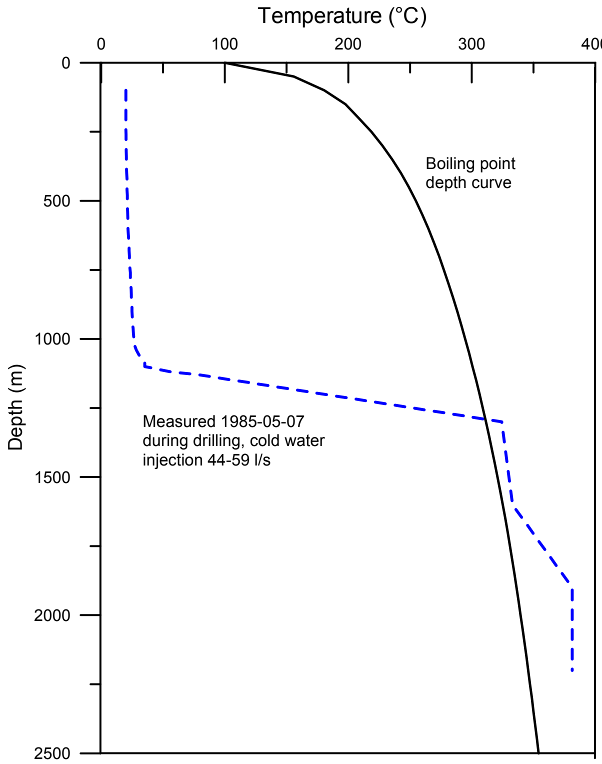

FIGURE 8: Temperature profile of well NJ-11 during underground blowout; the BPD curve for pure water is shown for comparison (Steingrímsson et al., 1990)

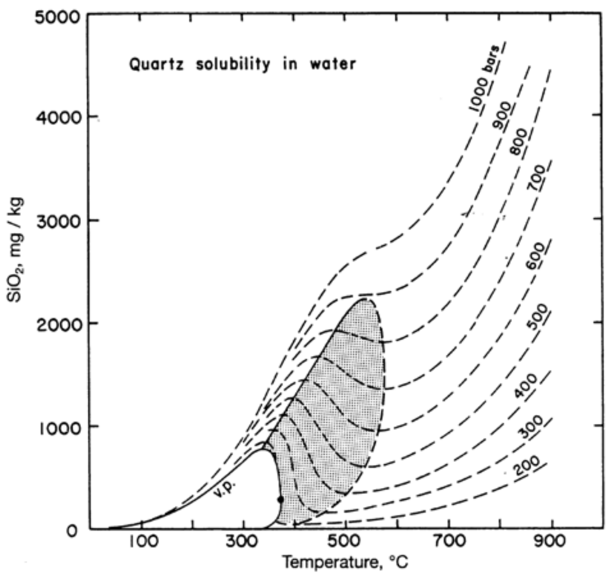

FIGURE 9: Calculated solubilities of quartz in water as a function of temperature along isobars ranging from 200 to 1000 bar. The shaded area shows a region of retrograde solubility in which the solubility of quartz decreases with increasing temperature at constant pressure (Fournier, 1985)

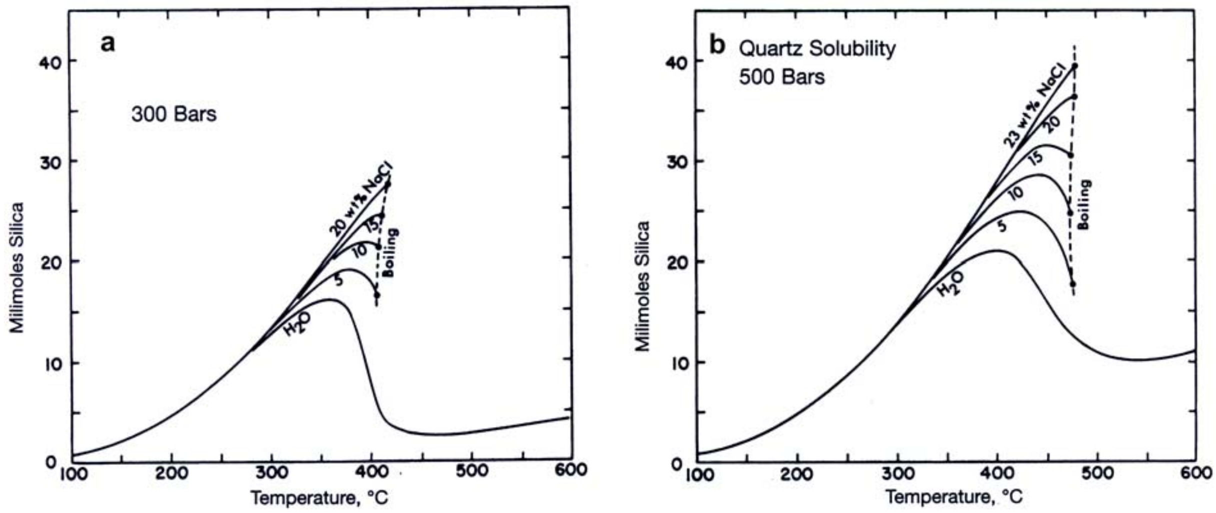

FIGURE 10: Comparsion of calculated solubilities of quartz in water and in NaCl solutions at; a) 300 bars; and b) 500 bars pressure (Fournier, 1983)

Coming at the brittle-plastic transition zone from the other direction (fluid moving from the higher P_f region in plastic rock into the lower P_f region in brittle rock), there is a large potential for the precipitation of silica from dilute and highly saline fluids with decreasing pressure at >400°C (Figure 10). Decompression is also likely to result in massive evaporative boiling of brine that causes additional supersaturation with respect to the solubility of quartz (Fournier, 1999).

In the above discussion emphasis was placed on quartz deposition as a major factor in the formation of a self-sealed zone because quartz veins commonly occur in hydrothermal systems. Other commonly observed veins minerals, including carbonates, sulfates, sulfides, oxides, and other silicates, may also play major roles in the development and/or reestablishment of a self-sealed zone.

The temperatures and pressures in such formations are impossible to estimate because self-sealed conditions are different over time and the temperatures and pressures in which the self-sealed zone was formed, and are also very complicated. When drilling into such conditions, the best way to estimate the temperature and pressure is to use measurement while drilling (MWD) tools to monitor the down-hole conditions.

The technical solution to overcome many of the problems posed by these cases is to case and cement the upper parts of the well before drilling into the supercritical zone.

3.3 Estimating bottom hole circulation temperatures while drilling

In drilling high-temperature wells, knowledge of accurate temperatures with circulating time has a direct bearing on drilling fluid rheology, its design, the determination of thermal stresses on tubular, the determination of casing depth and design of cementing programmes, logging tool design and log interpretation. The drill bit and other down-hole tools also have temperature-sensitive parts and temperature limitations (Table 2). Estimation of the well temperature profile while drilling is, therefore, important for success of the drilling project.

3.3.1 Temperature profiles in Iceland

Data from wells drilled in high-temperature fields all over the world suggest that the maximum temperature can be expected to follow the boiling point curve (BPD), based on the assumption of water at boiling conditions at any depth in the well (Figure11). Only a few wells drilled in the world are deep enough to have reached supercritical conditions.

TABLE 2: Maximum temperature rating of drilling tools and materials (from JAPEX)

	Max. Temperature (°C) 50 100 150 200 250 300 350 400	1985 Max.	1995 Max.	Develop. Target
Down hole motor				
PDM		135°C	175°C	240°C
Turbine		160°C	315°C	
Vertical drill. system		160°C	175°C	200°C
Core barrel		300°C	300°C	
MWD				
Standard type		125°C	150°C	175°C
Vert. drill. for KTB		125°C	175°C	200°C
Heat sealed type		260°C	260°C	
Cementing				
Shore, collar		150°C	210°C	
Stage cementer		135°C	135°C	
Cement with silica		400°C	400°C	
Cement additive		180°C	260°C	
Bit				
Sealed bearing		180°C	200°C	260°C
Natural diamond		650°C	650°C	
PDC		750°C	750°C	
TSP		1200	1200	
Drilling mud				
Water base mud		180°C	250°C	
Viscosifier		250°C	370°C	
Fluid loss reducer		230°C	230°C	
Dispersant		260°C	350°C	
Lubricant		200°C	300°C	
Drilling jar				
Hydraulic type		290°C	315°C	
Mechanical type		230°C	285°C	
Blow-out preventer		200°C	200°C	
BOP ram		85°	175°C	
CSG hanger seal		85°C	120°C	
Liner hanger		205°C	260°C	

3.3.2 Modelling the temperature profile and bottom hole circulation temperature

Model development. The estimation of circulation temperatures while drilling is important for the selection of bits and down-hole tools. Many approaches can be used to estimate well temperature, both numerical and analytical. There are several models and methods to calculate and analyse the formation temperature while drilling, for example, the Horner-plot method (e.g. Parasnic, 1971), a curve fitting method based on a numerical model (Chiba et al., 1988) or analysis of fluid inclusion (e.g. Fujino and Yamasaki, 1985). But all of these models and methods were basically used in low-temperature petroleum wells. Because the temperature is very high and there are usually more than two temperature gradients in the same well, it is much more complicated to estimate a geothermal well

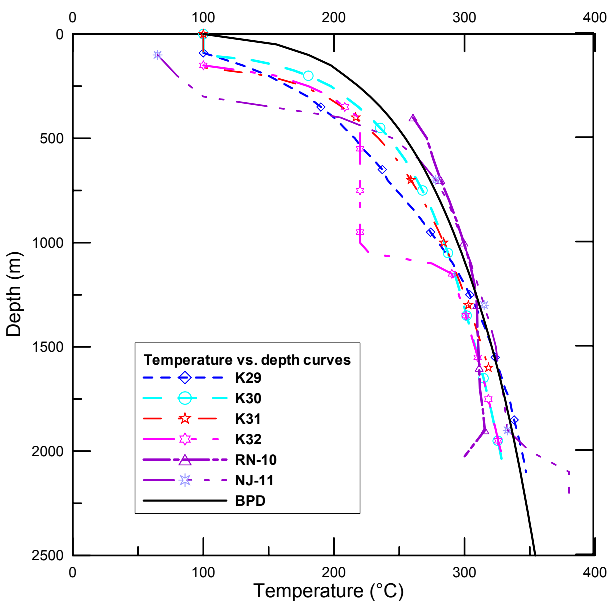

FIGURE 11: Temperature profiles in high-temperature geothermal wells in Iceland, K-Krafla, RN-Reykjanes, NJ-Nesjavellir

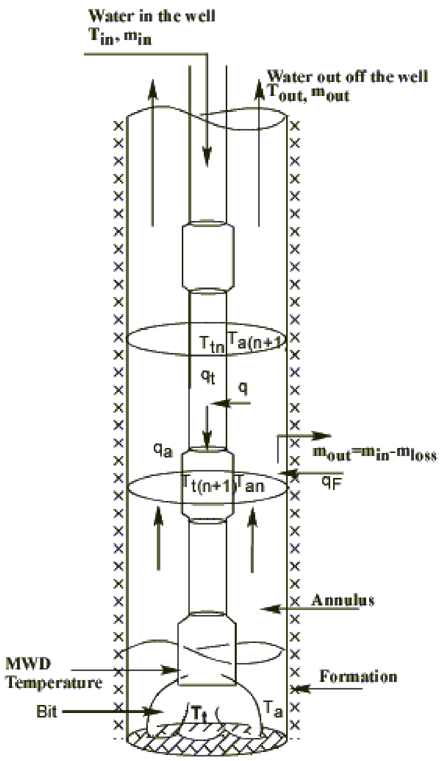

FIGURE 12: Circulation system of a well showing modelling parameters

temperature profile during drilling. For this study, we choose the STAR and GEOTEMP2 models to calculate and analyse the geothermal well temperature while being circulated.

STAR method. The STAR model was developed by Mr. Sverrir Thórhallsson and Dr. Árni Ragnarsson of Orkustofnun in the year 2000. The STAR name indicates the initials of the authors. This author contributed to its development verifying its accuracy by comparison with actual data.

The circulation system that exists in a well at any given time is shown in Figure 12. The heat-transfer rate for the fluid in the annulus depends both on the formation temperature and the drillpipe fluid temperature. The fluid is pumped into the drillpipe to the bottom of the hole and then returns through the annulus to the surface. The entering fluid temperature at the surface, the fluid inlet temperature, T_{in}, can be either higher or lower then the formation temperature at the surface. However, the formation temperature at bottom hole is much higher than that of the fluid entering the well. Thus, during flow down the drillpipe, the fluid generally gains heat from the annulus fluid which, in turn, is heated by the formation. A higher annulus fluid temperature means that it loses heat to the down-flowing fluid inside the drillpipe.

Heat flow from the formation to the annulus. The heat flow, per unit length of well, q_F (W/m), from the formation to the annulus is given by the following transition equation (Themie project GE-0060/96, 1998):

$$q_F = 4k_f\pi(T_f - T_a)\left(\ln\frac{4k_f t}{\rho_r c_r r_w^2} - 1.15\right)^{-1} \qquad (1)$$

where k_f = Thermal conductivity of rock [W/m°C];
T_f = Initial formation temperature [°C];
T_a = Annular water temperature [°C];
t = Circulation time [s];
ρ_r = Density of rock [kg/m^3];
c_r = Heat capacity of rock [J/kg°C];
r_w = Radius of the well [m].

In Equation 1, we set a circulation time, t, function. With longer circulation time, the heat flow from the formation to the annulus, q_F, decreases. That means when a well is being drilled continually, the q_F value changes at a certain depth as the circulation time increases. Figure 13 shows the q_F values as a function of different circulation times.

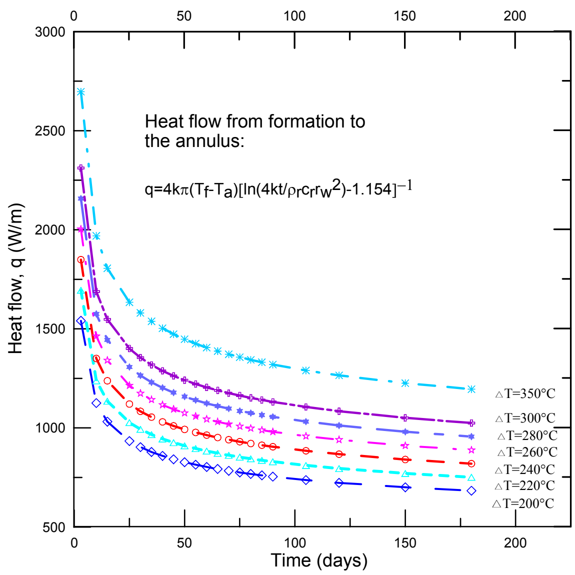

FIGURE 13: Heat flow from formation to annulus at different circulation times, by Equation 1

Heat flow from the annulus water to the drill pipe. The heat flow, per unit length of well, q (W/m), from the fluid in the annulus to the fluid inside the drillpipe can be calculated as follows:

$$q = U(T_a - T_i)dz \tag{2}$$

where U = Overall heat transfer coefficient between annulus and inside of drill pipe [W/m°C];
T_t = Fluid temperature inside the drill pipe [°C].

The overall heat-transfer coefficient, U, depends on the heat transfer coefficients on the inside and outside of the drill pipe as well as the thermal conductivity in the pipe wall. It can be calculated from the equation:

$$U = \frac{1}{R_1 + R_2 + R_3} \tag{3}$$

where R_1 = Thermal resistance outside the pipe;
R_2 = Thermal resistance of the pipe;
R_3 = Thermal resistance inside the pipe;

The thermal resistance outside the pipe; R_1 is defined as

$$R_1 = \frac{1}{h_1} = \frac{D}{Nu_i k_a} \tag{4}$$

with

$$D = d_w - d_{po} \qquad and \qquad Nu_i = 0.9 Nu (\frac{d_w}{d_{po}})^{0.45} \tag{5}$$

The Nusselt number, Nu, for heat transfer for this co-axial case is given as follows (VDI, 1963):

$$Nu = 0.037 \left[1 + (\frac{D}{L})^{2/3} \right] (Re^{0.75} - 180) Pr^{0.42} (\frac{\eta_f}{\eta_w})^{0.14} \qquad and \qquad Re = \frac{\rho_w \nu D}{\mu} \tag{6}$$

The thermal resistance of the pipe, R_2, is

$$R_2 = \frac{1}{h_2} \qquad and \qquad h_2 = \frac{2k_p}{d_{po} \ln(d_{po}/d_{pi})} \tag{7}$$

The thermal resistances inside the pipe, R_3, is

$$R_3 = \frac{1}{h_3} = \frac{D}{Nu k_i} \qquad and \qquad D = d_{pi} \tag{8}$$

where the variables in Equations 3-8 are defined as
d_w = Diameter of the well [m];
d_{po} = Outside diameter of the drill pipe [m];
d_{pi} = Inside diameter of the drill pipe [m];

Nu = Nusselt number;
Nu_i = Nusselt number (after correction);
k_p = Drill pipe thermal conductivity [W/m°C];
k_i = Thermal conductivity, water down flow [W/m°C];
k_a = Thermal conductivity, water up flow [W/m°C];
ρ_w = Water density, water down flow [kg/m^3];
ν = Water velocity [m/s];
μ = Dynamic viscosity of water [kg/ms];
Re = Reynolds number;
η_f = Dynamic viscosity of water at average water temperature [kg/ms];
η_w = Dynamic viscosity of water at wall temperature [kg/ms];
D = Characteristic length for the flow (diameter) [m];
L = Depth of the well [m];
Pr = Prandtl number of water.

Calculation of temperature profiles in the flow directions. Divide the well depth into many elements of equal length, 500 in this case, thus assuming that the changes of the temperature in the flow direction are very small within each element. In the beginning, we guess some value for the bottom hole temperature. By approximating the average fluid temperature in the lowermost element as equal to the bottom hole temperature, we can use the equations developed above to calculate the heat flow values for this element, q_F, from the formation to the annulus and q from the annulus to the drill pipe. A heat balance for each of the two flows, in the annulus and inside the drill pipe, is then used to calculate the temperature variations up the well.

For the flow in the annulus we have

$$q_F - q \;=\; m_{out} c_p (T_{an} - T_{a(n+1)}) dz \tag{9}$$

and for the flow inside the drill pipe we have

$$q \;=\; m_{in} c_p (T_{t(n+1)} - T_{tn}) dz \tag{10}$$

where m_{out} = Flow rate up the annulus [l/s];
m_{in} = Flow rate inside the drill pipe [l/s];
c_p = Specific heat of water [J/kg°C].

When the new temperature at the top of the lowermost element, T_{tn} and $T_{t(n+1)}$, has been calculated, we move to the next element and repeat the procedures discussed above. When the top of the well is reached, the calculated inlet water temperature to the drill pipe is compared with the actual temperature, T_{in}. The difference is used to make a new guess for the bottom hole temperature and the calculation starts from the beginning. This iteration procedure finally results in a drill pipe temperature at the top equal to the known inlet water temperature.

The boundary conditions of the method assume the formation temperature, T_f, follows the boiling point with depth curve (BPD) temperature; T_t=T_a at bottom of the hole. Other reservoir temperature profiles can also be entered in the program.

An important feature of the model is that annular flow (return) can be changed to reflect fluid losses at selected depths.

GEOTEMP2 program. GEOTEMP2 is a computer program, originally developed by Mondy and Duda (1984) to take into account lost circulation and convective flow within the formation. There are six options in the programme: injection, production, drilling, air drilling, mist drilling and steam production. Here we only use the drilling option to calculate and estimate the formation temperature.

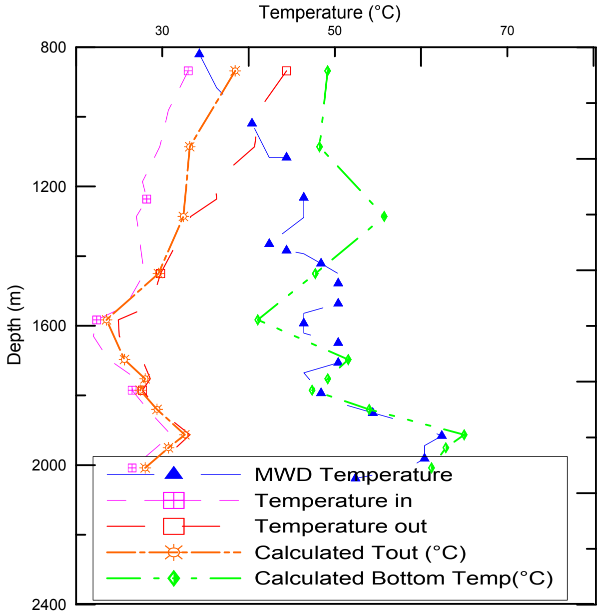

FIGURE 14: Well KJ-30 measured and calculated temperature curves (by the STAR program)

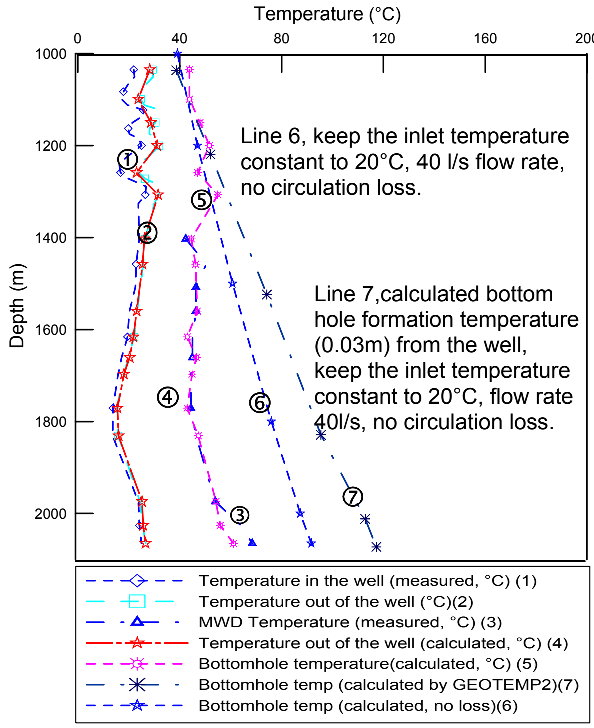

FIGURE 15: Well KJ-29 measured and calculated temperature curves by STAR and GEOTEMP2

3.3.3 Examination of the precision of estimated circulation temperature

In order to examine the precision of the estimated circulation temperatures by STAR and GEOTEMP2, data from two geothermal wells, KJ29 and KJ30, drilled in the Krafla high-temperature geothermal field in Iceland were compared with the calculated temperatures. Using the field data, and inputting the inlet temperature, flow rate and circulation losses according to depth (by the STAR model), a very good agreement with measured data was obtained (Figures 14 and 15). Giving the bottom hole formation temperature and temperature gradients (according to the BPD temperatures curve or the temperatures from a nearby well), and the drilling data, the results from the GEOTEMP2 show (Figure 15 - curve 7) that the calculated formation temperatures (0.03 m from the well) are higher than the actual MWD temperatures logged near the drill bit and also higher than the temperatures of the STAR model. Probably due to cooling by 5-20 l/s circulation loss in the well while drilling, the calculated temperatures of GEOTEMP2 are higher as the calculations are based on no circulation losses. The wellbore temperatures (at 0.03 m from the well) must also be a little bit higher than that of the annulus water.

3.3.4 Modelling well temperatures below 2000 m to 5000 m while drilling

Figure 16 shows the casing profile and drilling time estimated for a 5000 m deep well. According to the well design, it consists of three sections, 700-2300 m, 2300-3400 m and 3400-5000 m. In the first section, as many wells have been drilled to that depth, the well temperature distributions are well known during drilling. Thus, it is not necessary to estimate the bottom hole temperature for this section of the well.

In the 2300-3400 m section (12¼″ hole section), assuming that the initial formation temperatures follow the BPD curve, the inlet water temperature 20°C, flow rate 50 l/s. For this section the bottom hole circulation temperatures at different depths with 5-10 l/s circulation loss and without loss are calculated by using both STAR and GEOTEMP2 (Figure 17). Results by the STAR model show that the maximum bottom hole temperature will be 130°C at no circulation loss. Compared to well WD-1A drilled in Japan

(Figure 6), the estimated result is reasonable. In such situations, the bottom hole temperature is still acceptable for most of the downhole tools. The calculated temperatures by GEOTEMP2 are higher, or 200°C.

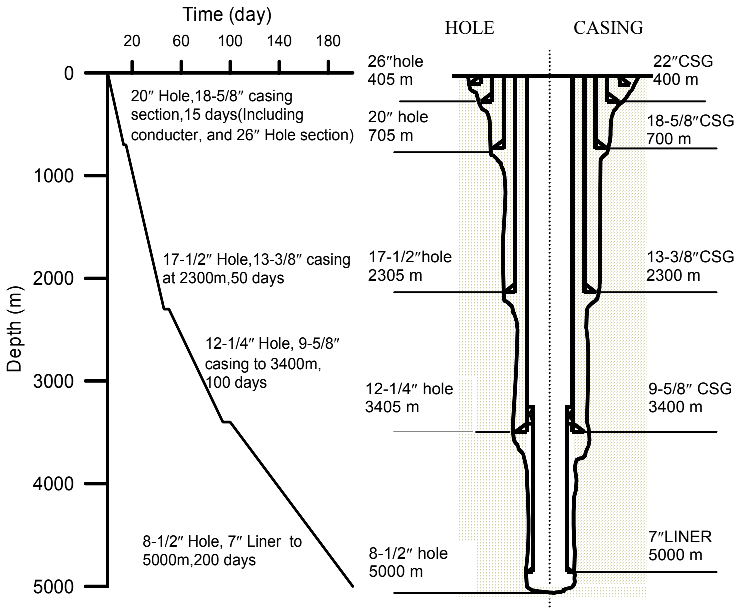

FIGURE 16: Estimating drilling time and casing profile

In the 3400-5000 m (8½″ hole) section, assuming that temperature reaches the critical point at 3500 m, the temperature gradient is assumed about 100°C/km, so the maximum formation temperature at 5000 m will exceed 500°C. Assuming the inlet temperature is 20°C, and the flow rate 40 l/s, the bottom hole circulation temperatures are calculated by both the STAR and the GEOTEMP2 program. The calculated results (Figure 18) show that if there is no circulation loss in this section, the bottom hole temperature will be 266°C (by STAR model). In this situation, the temperature will limit the use or reduce the life of some downhole tools. To prevent the downhole tools from being cooked in the well, the TDS (top drive system) is recommended for use. The GEOTEMP2 gives a very high bottom temperature, about 350°C at 5000 m. Of course, if the well has a circulation loss somewhere, 5-10 l/s loss for example, the bottom temperature will decrease very rapidly.

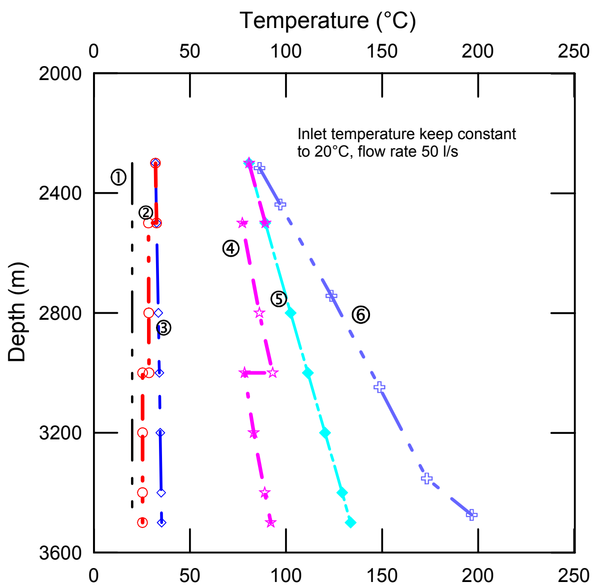

Line (1), Inlet temperature (°C)
Line (2), Outlet temperature (°C), with a circulation loss 5 l/s at 2500m, another loss 5 l/s at 3000m.
Line (3), Outlet temperature (°C), no circulation loss.
Line (4), Bottom hole temperature (°C),with a circulation loss 5 l/s at 2500m, another loss 5 l/s at 3000m.
Line (5), Bottom hole temperature (°C), no circulation loss.
Line (6), Calculated bottom temperature(0.03m from the well) by GEOTEMP2, no circulation loss (°C)

FIGURE 17: Modelling the circulation temperature by STAR and GEOTEMP2 models (2300-3500 m)

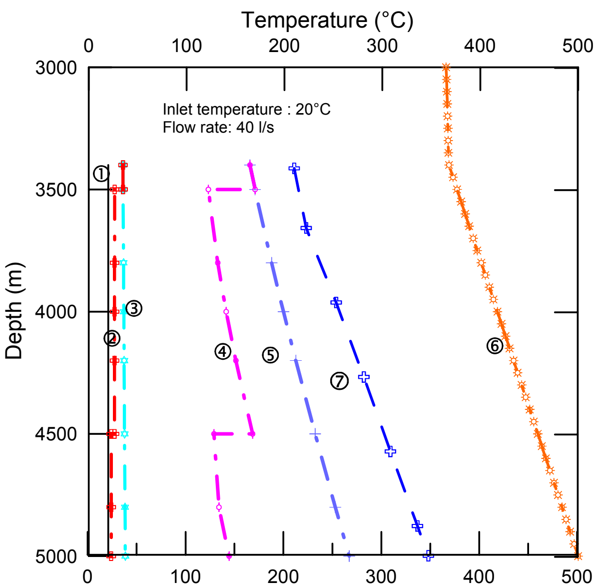

Line (1), Inlet temperature (°C)
Line (2), Outlet temperature (°C), with a circulation loss 5 l/s at 3800m, another loss 5 l/s at 4500m.
Line (3), Outlet temperature (°C), no circulation loss.
Line (4), Bottom hole temperature (°C),with a circulation loss 5 l/s at 3800m, another loss 5 l/s at 4500m.
Line (5), Bottom hole temperature (°C),without circulation loss.
Line (6), Initial formation temperature, BPD curve to 3400m, another temperature gradient to 5000m
Line (7), Bottom hole temperature (°C),calculated by GEOTEMP2, without circulation loss.

FIGURE 18: Modelling the circulation temperature by STAR and GEOTEMP2 models (3500-5000 m)

3.4 Casing strength and casing design

3.4.1 Thermal stress behaviour under cyclic steam-stimulation conditions

Changes of temperature during drilling operations or production or killing the well may result in severe stresses, and sometimes in failure of the casing, particularly in axial compression. In a high-temperature geothermal well, when the casings have been run into the well and then heated, the casing is subjected to a period of heating during the heating up phase, and a cooling period during subsequent circulation or killing of the well. When casing is heated up or cooled down, one of two things will happen: the casing will either expand or contract if allowed to do so. If the casing is fixed at both ends, as when the casing is cemented from bottom to surface, then compressive and tensile stresses are generated as the pipe is not free to move. These stresses may be large enough to exceed the pipe yield strength or the coupling joint strength, resulting in casing failure. Steam temperatures as high as 400-500°C, and pressures up to 200 bars have been reported in some geothermal wells. If the temperature is high enough, the yield strength of the casing materials will be exceeded and the casing will become plastically deformed. Therefore, during the well heating phase, the casing may fail as a result of plastic deformation and the connections may fail as a result of excessive compressive load. When the casing is cooled, the tensile stress generated may be high enough to cause tensile failure of the pipe or the connection. When the casing is cooled to its original temperature (as before heating), a permanent residual tensile stress will be left in the casing. In addition to creating the potential for tensile failure, this residual tensile stress causes the casing to be more susceptible to biaxial collapse failure.

Maruyama et al. (1990) conducted a series of experiments to investigate the behavior of casing pipe body and connections under stimulated thermal recovery conditions. The study examined the thermal stress behaviour and leak resistance of pipe and connections at temperatures up to 354°C under severe loading conditions similar to those encountered in thermal wells. They also studied the biaxial collapse resistance of the casing under the large axial tension force that would exist after the cooling period in a steam-stimulation process.

Figure 19 shows a typical thermal-load vs. temperature diagram for 178 mm, 34.2 kg/m Grade K55 casing undergoing cyclic steam stimulation. The figure shows load vs. temperature at a final cycling temperature of 354°C after the test sample had previously been subjected to thermal cycling at 250 and 300°C (Maruyama et al., 1990).

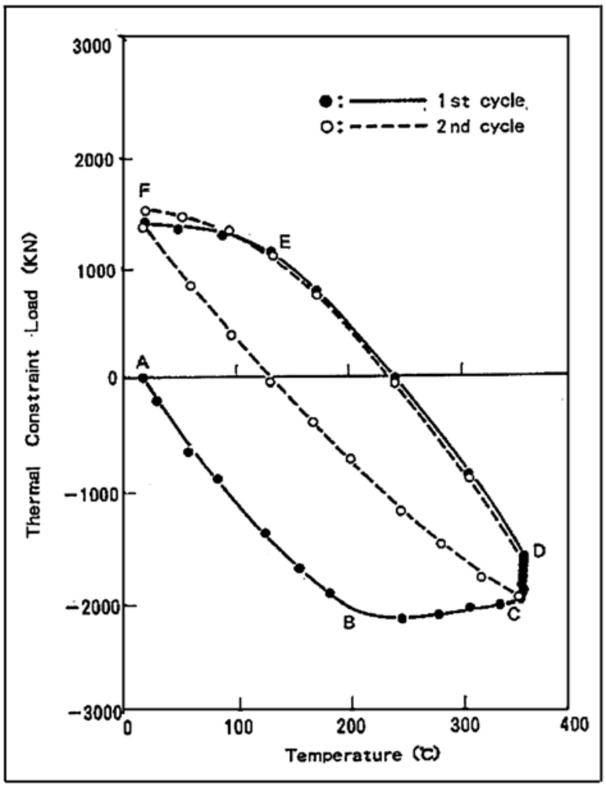

FIGURE 19: Typical cyclic thermal load history of work-hardening material 7", 34.2kg/m K55 casing (Maruyama et al., 1990)

Path AB shows that the elastic response of the material in which compressive load is developed in proportion to the temperature change. The compressive load may be calculated by Equation 11

$$L_T = E(K\Delta T)A \tag{11}$$

where L_T = Temperature-generated load in pipe [kN];
E = Young's elastic modulus, E = 20.6 MPa;
K = Coefficient of linear expansion (1/°C), K= 10^{-5} /°C for steel;
ΔT = Temperature change [°C];
A = Pipe cross-sectional area [mm].

From the thermal load response presented in Figure 19, it is apparent that the amount of residual tensile load (Point F) depends strongly on the degree of plastic yielding (path BC) and the amount of stress relaxation (path CD). A larger temperature range over which plastic yielding occurs results in a larger amount of residual tensile load. Also, a larger amount of stress relaxation results in a greater residual tensile load.

3.4.2 Effect of temperature, heating cycle, and casing grade on thermal load behaviour

Figure 20 shows thermal load vs. temperature for 178 mm, 34.2 kg/m Grade K55 casing at three temperatures. Three new findings, however, resulted from the temperature and heating cycles. First, the maximum tensile and compressive loads at 300 and 354°C were essentially the same, even though plastic deformation at 354°C was larger than that at 300°C. This suggests that if a significant plastic deformation existed, the maximum compressive and tensile load would be the same, regardless of the temperature difference. Second, the amount of stress relaxation increased with temperature. It ranged from 200 kN at 250°C to 400 kN at 354°C. Third, the elastic limits in compression at 300 and 354°C were about 300 kN larger than those at 250°C. Thus, the prestrain buildup in the casing in the first heating cycle increased the elastic limit of the casing during subsequent heating cycles because of strain aging. Hence, Grade K55 casing will actually become stronger in the second and subsequent heating cycles in a cyclic steam-stimulation operation. In fact, after undergoing both work hardening and strain aging, Grade K55 casing will acquire a compressive yield strength as large as that of Grade L80 casing.

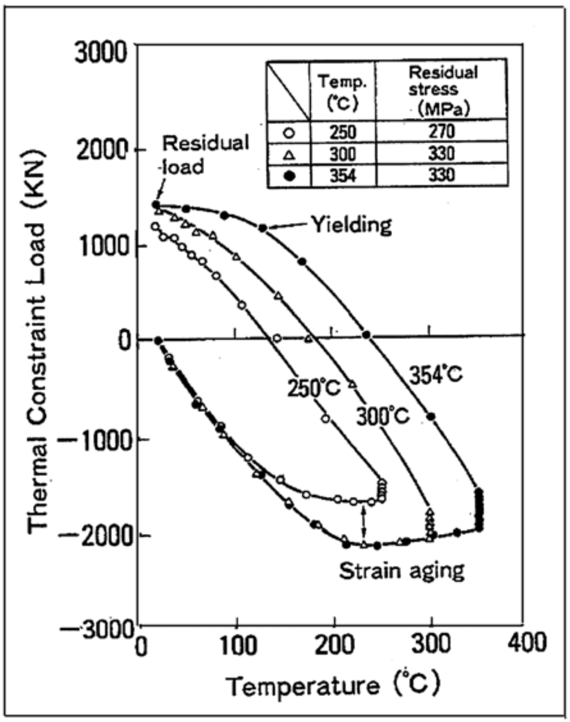

FIGURE 20: Effect of temperature on the cyclic thermal load history of work-hardening material 7", 34.2kg/m K55 casing (Maruyama et al., 1990)

Table 3 summarizes the residual tensile stresses obtained from the thermal simulation tests for Grades K55, L80, and C95 casing (Maruyama et al., 1990).

TABLE 3: Residual tensile stress for different casing grades (MPa)

Casing grade	Temperature (°C)		
	250	**300**	**354**
K55	270	330	330
L80	190	350	500
C95	88	275	549

3.4.3 Collapse pressure with axial tensile load

Quenched-and-tempered casing and as-rolled casing showed significantly different collapse-resistance characteristics under tensile load. Figure 21 shows the measured collapse pressure of Grade N80 casing, which is a quenched-and-tempered material. The solid line is the collapse resistance predicted by Equation 12, a modified version of the API collapse equation based on the von Mises yield criterion:

$$P_{ya} = \left[\sqrt{1 - 0.75(\sigma/s)^2} - 0.5(\sigma/s)\right] p_{yi} \tag{12}$$

and

$$P_{yi} = 2s(d/h - 1)/(d/h)^2 \tag{13}$$

where P_{ya} = Biaxial collapse pressure [MPa];
P_{yi} = Pipe internal yield pressure [MPa];
d = Pipe OD [mm];
h = Pipe wall thickness [mm];
s = Pipe yield strength [MPa];
σ = Axial stress applied to pipe [MPa].

Note that the measured collapse pressures (Figure 21) are in good agreement with those predicted by Equation 12. Figure 22 shows the measured collapse pressure for the Grade K55 casing, as-rolled material. The solid line is the collapse pressure predicted by Equation 12. Note that at low axial stresses, the measured collapse pressures are in good agreement with those predicted by the API equation. At high axial stresses, however, the measured collapse pressures are significantly higher than those predicted by the API equation. This deviation is caused by the work-hardening nature of Grade K55 casing.

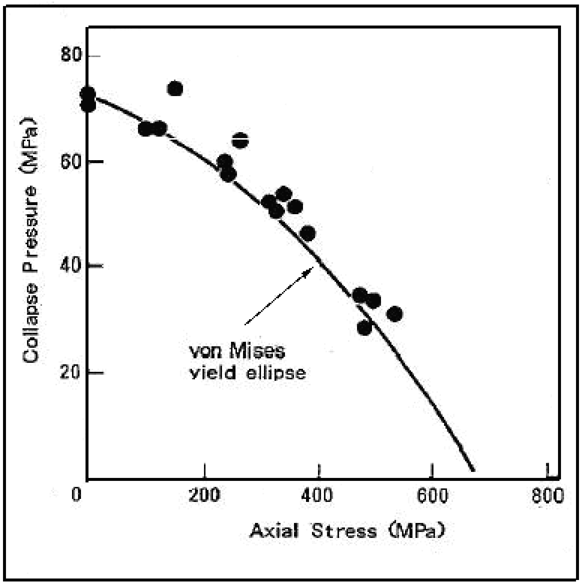

FIGURE 21: Biaxial collapse resistance of 7", 38,7 kg/m N80 casing (Maruyama et al., 1990)

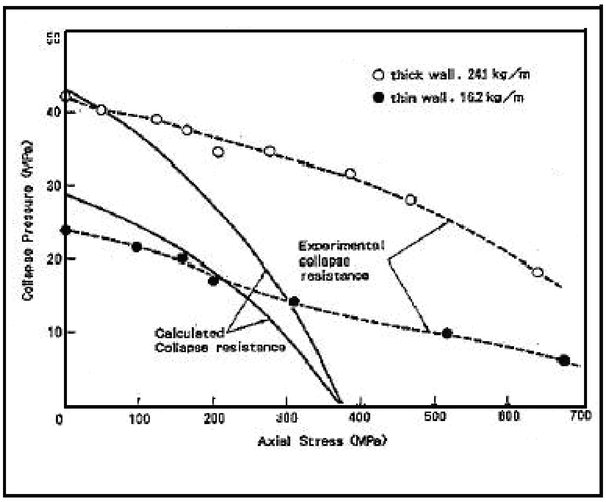

FIGURE 22: Biaxial collapse resistance of 7", 38,7 kg/m K55 casing (Maruyama et al., 1990)

We may conclude that the biaxial collapse pressure depends on stress/strain characteristics of the material. For the quenched-and-tempered material, a perfect elastic/plastic material, the biaxial collapse pressure is predicted adequately by the API equation. Because Grades L80, C95, and P110 casings are all quenched-and-tempered material, we expect that their biaxial collapse resistance can be predicted by the API equation. For the as-rolled material, a work-hardening material, the biaxial collapse resistance is much higher than that predicted by the API equation. It seems reasonable to take advantage of the work-hardening characteristic of the as-rolled material in designing thermal wells.

3.4.4 Mechanical properties of casings used in geothermal wells

Tensile properties. Casings used in geothermal wells are manufactured in accordance with API specifications. These specifications furnish no minimum strength requirements at elevated temperatures, but list tensile properties at room temperatures for the various API grades of casing, as listed in Table 4 (API specification 5CT, 1992).

TABLE 4: Tensile requirements of casing pipe manufactured in accordance with API specification 5CT

Casing (grade)	Yield min. (kg/mm^2)	Strength max. (kg/mm^2)	Min. tensile strength (kg/mm^2)	Min. elongation (% in 2")
H-40	28.1	-	42.2	29.5
J-55	38.7	56.2	52.7	24.0
K-55	38.7	56.2	66.8	19.5
C-75	52.7	63.3	66.8	19.5
N-80	56.2	77.3	70.3	18.5
P-110	77.3	98.4	87.9	15.5

Elongation - all groups. The minimum elongation in 2 inches shall be determined by the following formula (API specification 5CT, 1992):

$$e = 625{,}000 \frac{A^{0.2}}{(U/14.5)^{0.9}} \tag{14}$$

where e = Minimum elongation in 2 inches in percent rounded to nearest ½ percent;
A = Cross-sectional area of the tensile test specimen in square inches, based on specified outside diameter or nominal specimen width and specified wall thickness, rounded to the nearest 0.001 sq. in., or 0.75 sq. in., whichever is smaller;
U = Specified tensile strength [bar].

For high-temperature geothermal wells, the maximum temperature in the well could reduce the strength and other properties of steel casing materials. The design of a high-temperatures well should be based on the reduced values. The data furnished by the casing manufacturers for room temperature are not applicable to the high-temperature geothermal wells.

Figure 23 shows the design yield strength reduction due to increased material temperature (Snyder, 1979). The modulus of elasticity also decreases from about 30×10^6 psi at 25˚C to 27×10^6 psi at 371˚C and seems to vary little for various steels (Nicholson, 1984).

Thomas (1967) reports on tests made at elevated temperatures on various grades of API casing from four different manufactures. The results of these tests are shown in Figure 24, showing the relative change in yield and tensile strength of the pipe at different temperatures. The relative change of tensile strength turns out to be fairly consistent for all grades of casing. The average change is shown in Figure 24.

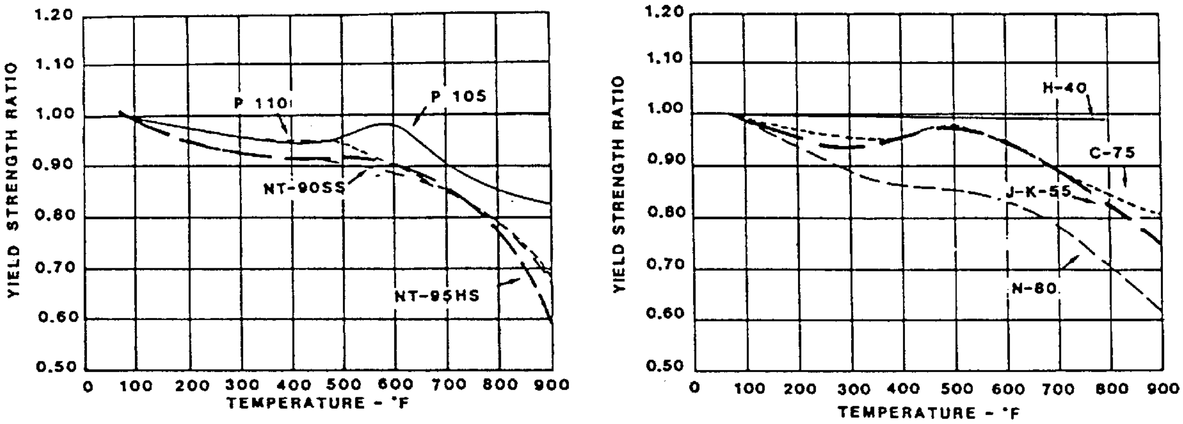

FIGURE 23: Yield strength ratio curves for indicated steel casing materials at elevated temperatures (Nicholson, 1984)

Based on this information it seems safe to assume that the tensile strength of casing is unchanged up to a temperature of about 350°C. This is in accordance with tensile strength values at elevated temperatures for seamless pipe of various grades of ASTM steels (The American National Standards, 1973).

For safe design the reduction in relative yield strength of casing is assumed to be the maximum reduction as listed by the DIN code for St.45.8. The same relative reduction is assumed to apply to all grades of casing giving the following relationship between yield strength and temperature.

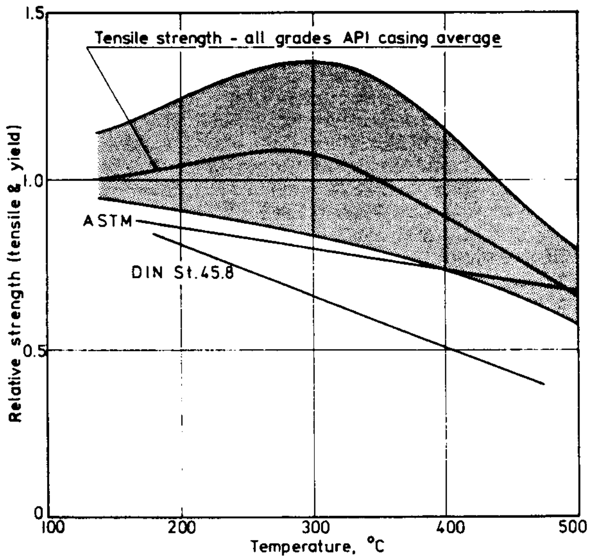

FIGURE 24: Variation in relative strength limits (tensile or yield) for API casing. The shaded area denotes the range of yield strength obtained for various grades of casing (Karlsson, 1978)

$$Y/Y_o = \begin{cases} 1 & for \quad T \le 80\,°C \\ (1-(T-80)/640 & for \quad T > 80\,°C \end{cases} \qquad (15)$$

where Y_0 = Minimum yield strength in room temperature condition as give in Table 4.

The tensile strength of API casing is assumed to stay unchanged up to a temperature of 350°C. This is in accordance with listed values for seamless pipe material made by U.S. Standards. When temperature is high, up to 350°C, and with increasing temperature, the tensile strength decreases. This assumption is also supported by test data described in Thomas (1967) and Karlsson (1978).

3.4.5 High-temperature design stress intensity

For a high-temperature well, the design stress intensity is defined as the lowest of the following stress values:

a. One third of minimum tensile strength at room temperature;
b. One third of minimum tensile strength at working temperature;
c. Two third of minimum yield strength at room temperature;
d. Two third of minimum yield strength at working temperature.

With the tensile properties of API casing listed in Table 4, and reduction in yield strength at elevated temperature as given by Equation 15, the design stress intensity for various grades of casing are listed in Table 5 (Karlsson, 1978).

TABLE 5: Design stress intensity, S_m, kg/mm^2, for API casing at elevated temperatures (Karlsson, 1978)

Temperature (˚C)	H-40	J-55	C-75	N-80	P-110
40	14.1	17.6	22.3	23.4	29.3
200	14.1	17.6	22.3	23.4	29.3
220	14.1	17.6	22.3	23.4	29.3
240	14.1	17.6	22.3	23.4	29.3
260	13.5	17.6	22.3	23.4	29.3
280	12.9	17.6	22.3	23.4	29.3
300	12.3	16.9	22.3	23.4	29.3
320	11.7	16.1	22.3	23.4	29.3
340	11.1	15.3	20.9	22.2	29.3

3.5 Casing design

3.5.1 Casing depth

In general, the casing programme of high-temperature geothermal wells in Iceland has, in the past, been approximately as listed in Table 6. Large diameter casing programmes with a 13⅜" production casing are also common.

TABLE 6: Casing programme for high-temperature geothermal wells in Iceland

Casing string	Depth range (m)	Hole dia. (inch)	Casing OD (inch)
Surface	30-70	22	18⅝
Intermediate	150-400	17½	13⅜
Production	700-1000	12¼	9⅝
Perf. liner	1500-2500	8½	7

Basically, the casing depth design, the minimum depth to which each casing string is set, is determined by the maximum pressure to be expected in the well. But there are many other aspects and particular geological conditions to be considered:

1. The depth of the open hole should be limited to avoid the exposure of the well to conditions which could be expected to lead to blowouts, not only at the surface but also underground;
2. Rock type or formation, including the location of any specific stratigraphic marker beds;
3. Compressive strength of rock, or at least its degree of consolidation;
4. Faulting, fracturing and gross permeability;
5. Different pressure system and its depth;
6. Any effects on drilling activities on the formation;
7. Fields types (steam-dominated, two-phase, water-dominated);
8. MWD log or LWD log data which can provide instant information about the well and the formation being drilled.

TABLE 7: Suggested casing programme for a deep high-temperature geothermal well

Casing string	Depth (m)	Hole diam. (inch)	Casing OD (inch)
Surface	70	30	26
Intermediate	400	24	22
Intermediate	700	21	18⅝
Intermediate	2300-2500	17½	13⅜
Production	3400-3450	12¼	9⅝
Perf. Liner	4000-5000	8½	7

For the IDDP deep geothermal well, the suggested casing depth design is shown in Table 7. Here the 22" casing is to be set at 400 m. The purpose is to case off the upper loss of the circulation zone. In this section, the water temperature exceeds 100˚C. That can lead to blowouts. In an active reservoir at 500-600 m depth, some 5-10 bar over pressure was reported in some wells. For the safety drilling, the 18⅝" casing must be run and this section cemented. Experience suggests that the reservoir at Reykjanes is intersected down to 1900-2200 m depth, where the water temperature exceeds 300˚C. Many loss circulations, zones will be encountered during drilling. Running and cementing the casing successfully will improve the opportunity for the next section to be drilled. Before drilling into supercritical condition, the production casing, 9⅝" casing, must be run and all the weak zones cemented off. According to the BPD temperature and pressure, the supercritical zone will be encountered below 3500 m, so the production casing must be set to 3400-3450 m, 100 m above the supercritical zone. Good cement is also required. Supercritical fluid higher than 220 bar, and temperature higher than 370˚C will be encountered. The powerful fluid can lead to dangerous blowouts if we fail to run the casing and cement the casing soundly.

3.5.2 Casing loads

Loads on a well casing may be of various types and occur during the running of the casing, cementing, and drilling. The subsequent string loads on the casing occur after completion of the well. These loads may occur both in the axial direction of the casing (tension and compression) or in the radial direction, inwards (collapse) or outwards (burst).

Axial loading before and during cementing. Until the annular cement sets around the casing, the tensile force at any depth should include the weight in the air of the string below, minus the buoyant effect of any fluid which may collect in the well. It is given by (New Zealand Standard, 1991):

$$F_p = \left(L_z W_p - \frac{L_f A_p}{n \times 10^3} \right) g \times 10^{-3} \tag{16}$$

where F_p = Tensile force at surface from casing weight, [kN];
L_z = Length of liner or depth of casing below any level, [m];
W_p = Nominal unit weight of casing, [kg/m];
L_f = Depth below liquid level, [m];
A_p = Cross-sectional area of pipe (mm^2), allowing for any slotting;
n = Mean specific volume of hot fluid, [l/kg];
g = Acceleration due to gravity, [9.81 m/s^2].

The design tensile force shall allow for dynamic loads imposed during the casing runs. Those loads may result from acceleration as the casing string is raised from rest to hosting speed, or deceleration due to braking. Because very severe shock loading can be generated when the string is stopped suddenly, such as by lowering the string quickly to the slips, this practice is forbidden, and does not need to be considered in casing design.

When running casing, the drag force of the casing against the side of the well, particularly in directional wells or in crooked holes, is an alternative to the acceleration loads described above. The casing should be designed to withstand axial dynamic forces which should be limited by specifying the maximum hook load which may be applied.

In a crooked hole, the maximum bending stress induced is (New Zealand standard, 1991):

$$f_b = 0.5282 E q D \times 10^{-3} \tag{17}$$

where f_b = Maximum stress due to bending, [Mpa];
E = Modulus of elasticity, [Mpa];
D = Outsider diameter of pipe, [mm];
q = Curvature [degree / 30 m].

The design tensile should also include any pretensioning of the upper section of the casing after anchoring the shoe, in order to reduce later compressive stresses due to heating.

The above axial loading applied before cementing should be added together where they can apply simultaneously. The safety factor is given by

$$\frac{\textit{Minimum tensile strength}}{\textit{Maximum tensile load}} \geq 1.8 \tag{18}$$

Axial load after cementing. The axial force imposed on casing after cementing should be checked by the equation (New Zealand Standard, 1991):

$$F_c = 2.4(T_2 - T_1)A_p \times 10^{-3} \tag{19}$$

The resultant force is

$$F_r = F_c - F_p \tag{20}$$

where F_c = Compressive force due to heating, [kN];
T_1 = Neutral temperature, [˚C];
T_2 = Maximum expected temperature, [˚C];
F_r = Resultant force, (kN].

The corresponding safety factor is:

$$\frac{\textit{Minimum compressive strength}}{\textit{Resultant tensile load}} \geq 1.2 \tag{21}$$

where the minimum strength refers to the lesser one of the pipe body or joint, respectively. The safety factor shall be not less than 1.2.

Of the various possible load combinations acting on the casing string, the most critical seem to be caused by external pressure and thermal expansion and by cementing with the inner-string method (collapse).

3.5.3 Internal pressure and thermal expansion

It is assumed that temperature and pressure in the well corresponds to boiling conditions. According to the ASME Code, the internal pressure and thermal expansion results in both primary and secondary stresses. Since a given pressure is always accompanied by a given temperature, the maximum pressure that a pipe of a given thickness can withstand may as well be given by the corresponding temperature. This is done in Table 8 for standard API casing (Karlsson, 1978).

TABLE 8: Maximum allowable temperature for API casing based on internal pressure (Karlsson, 1978)

Weight (lbs/ft)	H-40	J-55	C-75	N-80	P-110
32.3	275				
36.0	284	303			
40.0		313	326	331	
43.5			333	338	>340
47.0			339	340	>340
53.5			340	>340	>340
48.0	264				
54.5		288			
61.0		298			
68.0		306	322		
72.0			327	331	>340

If the temperature through the pipe wall is assumed to be constant and expansion of the pipe in the axial direction is prevented altogether, the maximum allowable temperature as prescribed by the Code is given by Table 9 for the various API casing grades. It has been assumed that the temperature can fluctuate from 40˚C up to a maximum. If the formation surrounding the casing in the well allows an axial expansion, the resulting maximum temperatures are considerably higher as shown in Table 9.

TABLE 9: Maximum allowable temperature for API casing based on axial expansion (Karlsson, 1978)

Axial expansion	H-40	J-55	C-75	N-80	P-110
None	222	270	320	340	>340
20%	262	312	>340	>340	>340

The results in Table 9 shows that even relatively limited expansion of the pipe considerably improves the capacity of the pipe to withstand high temperatures. It must be emphasized, however, that these results are based on the assumption of an integral casing string. This brings our attention to the screwed casing joints normally used for making up the string. According to the ASME Code, the range of stress intensity allowed for such joints is only one third to one half of that allowed for integral pipe. For this reason it is to be expected that cyclic thermal loads will cause failure of screwed casing joints (Karlsson, 1978).

3.5.4 Wellhead

The wellhead is an important part of the well design. For this deep geothermal well, the wellhead and valves must be capable of withstanding the powerful supercritical fluid during drilling and production. If you calculate the energy content of one kilogram of supercritical water, it is nearly equal to one kilogram of an explosive. But the wellheads now used in Iceland are not strong enough to withstand such powerful energy. A new wellhead which can handle over 300 bar pressure and temperatures over 500˚C needs to be developed.

3.6 MTC cement

For casing design, the standard practice is to design the casing while ignoring the cement effects. This is despite industry's acknowledgement that there is indeed a positive cement effect on the required strength of casing. A competent cement sheath, filling the annulus between casing and the borehole wall, significantly increases the burst resistance of the casing. The ballooning of the casing is constrained by the coupled formation and cement system. This constraining effect decreases the effective stress within the casing by transferring radial stress to the cement and formation, lowering the tangential stress within the pipe.

Cementing of casing is a crucial operation for any type of well. Failure of proper placement of the designed slurry usually results in expensive remedial work or damage of the casing during subsequent drilling and production or even loss of the well. In high-temperature geothermal well cementing, the higher the temperature, the more critical the problems to be overcome to achieve a successful cement job.

Present geothermal cementing equipment and practices have been adapted from the petroleum industry. But geothermal well cement is much more complicated than petroleum well cement. Not only due to high temperature, geothermal wells in general involve many weak formations (or lost circulation zones), from which cement slurry may leak and cause a cementing failure. A cementing failure may occur where gaps between the borehole and casing are not filled with cement; subsequent heating may lead to a break in the casing or underground blowouts. For a high temperature deep geothermal well, the deeper the well, and the higher the temperature, the more difficult the cement job is.

To prevent such failure, operators may use a lightweight cement slurry or multi-stage cement techniques. However, conventional lightweight cement slurry, (foam cement, microspheres or perlite lightweight additives) or multi-stage cementing techniques have the following problems:

- Low compressive strength;
- Diminished strength at high temperature;
- Complicated cementing operations.

A lightweight cement slurry with high strength at high temperature can bring about the following effects:

- Prevention of cement slurry leaks into fragile formations;
- Prevention of a casing collapse;
- Achieve cement returns;
- Reduce additional work.

The conventional cementing techniques can lower the cement slurry weight to 1.45g/cm^3, but will reduce the cement compressive strength, and the quality of the cement bond may not be very satisfactory for deep casing cement.

Mud-to-cement (MTC) is a new cementing technique developed by the petroleum industry in China. The Dian Quan Gui Drilling Company of SINOPEC, CHINA has performed hundreds of petroleum well cementing jobs with the MTC cement technique, including directional wells and horizontal wells and one intermediate-temperature geothermal well; the deepest well exceeds 4500 m in depth. The temperature is as high as 154˚C. The advantage of the MTC cement is the excellent quality of the cementing bond (Figure 25) and low price of the cement. The weight of MTC cement slurry is adjustable (Table 10) according to requirements from 1.25g/cm^3 to 1.90g/cm^3. The strength of MTC cement is much stronger than that required by the API standard. Figure 26 shows the MTC slurry lab test strength at 24 hours, 60˚C for different MTC slurry densities. When lowering the density to 1.25 g/cm^3, the strength of MTC exceeds 8.3 Mpa. It is still much better than the strength of any kind of conventional light-weight cement. The execution of the cement job is quite simple. The MTC slurry can be mixed in mud tanks before pumping into the well. Instead of cement trucks, the mud pump can also be used to implement the cement job.

TABLE 10: MTC slurry lab test data

Weight (g/cm³)	**Temp.** (˚C)	**Mobility** (cm)	**Thickening time** (min)	**Jelling time** (min)	**API water loss** (ml)	**24h/60˚C strength** (MPa)
1.25	45-80	22-28	85-200	50-190	215-700	8.3-12.5
1.45	45-90	22-28	68-310	40-350	200-500	10.8-13.7
1.70	45-100	23-27	110-240	55-200	151-400	13.6-17.9
1.80	20-120	22-26	100-300	55-270	120-300	14.2-20.8
1.90	20-120	22-24	150-311	70-300	80-260	18.6-24.8

Note: This test data is used for petroleum well cement

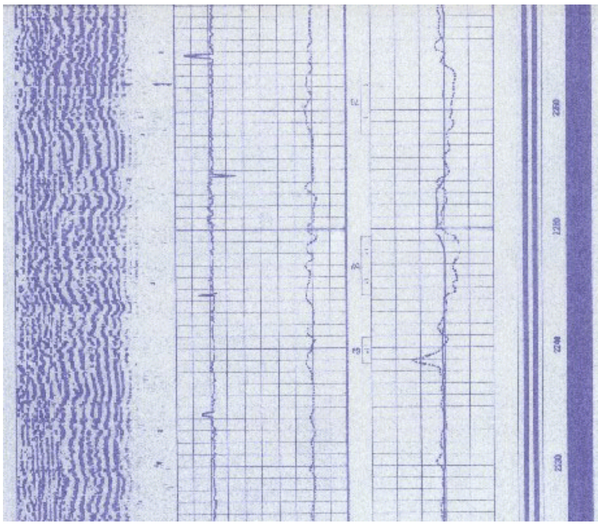

FIGURE 25: CBL logs with MTC cement for a petroleum well (from 2180-2230 m)

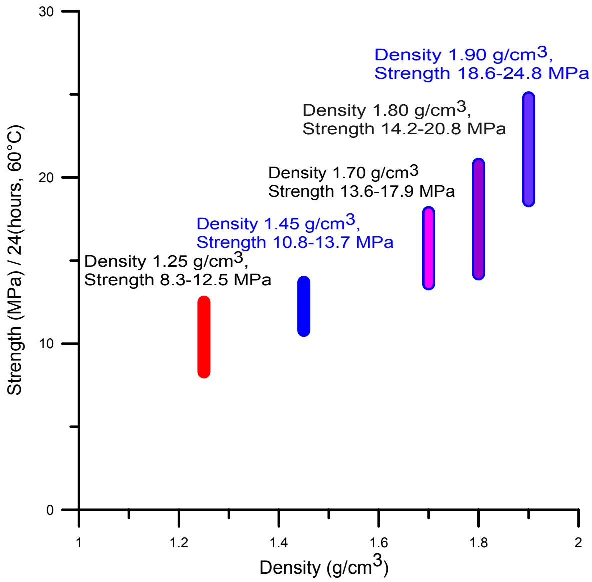

FIGURE 26: MTC slurry lab test strength (24 hour, 60˚C) for different slurry densities

For the MTC cement, the slag is the main material instead of conventional cement. Slag is a by-product of the steelworks. The chemical components of slag are CaO, SiO_2, AL_2O_3, and Fe_2O_3, MnO etc. Chemical additives such as dispersant´s synthesis, activating agent, fluid loss additive, retarder, antifoaming agent and mud are used in the mix. So far no high-temperature well has been cemented with the MTC technique, but experiments at high temperatures using the MTC technique will be completed soon. In the future, the MTC cement is likely to substitute the conventional cement mixes in geothermal wells.

3.7 Cooling the well and increasing the bit life with TDS

Top Drive Systems (TDS) is an advanced drilling system used extensively in petroleum drilling. In the geothermal area, the JMC Geothermal Engineering Co. Ltd, a Japanese company, used this system in drilling well WD-1A. In high-temperature drilling, many downhole tools have temperature sensitive parts and temperature limitations (Table 2). How best to cool the well during trips is a subject of interest. Using conventional cooling methods to drill high-temperature wells is a time consuming job. A new method was adopted to protect O-ring seals of the bit and other downhole tools from damage by high temperatures while running in the hole. The TDS cooling method is simply to lower the string at a controlled rate into the hole and pumping drilling fluid continuously while running the bottom-hole-assembly (BHA) into the hole by using the top-drive-drilling-system (TDS). This is not possible on a conventional rotary rig when the kelly is not connected.

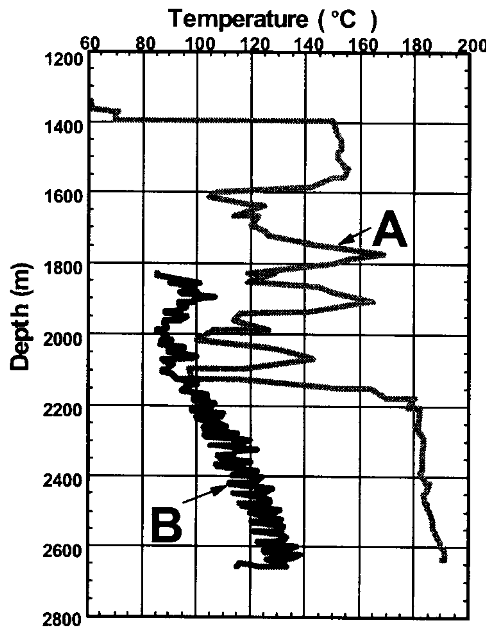

FIGURE 27: Borehole temperature curves of well WD-1A, recorded by PT-memory tools with and without pumping mud while running BHA into the hole. A: without pumping water (from 16.3 to 18 elapsed hours); B: pumping water with TDS (from 42.8 to 47.3 elapsed hours) (Saito and Sakuma, 2000)

To evaluate this TDS-cooling method, the New Energy and Industrial Technology Development Organization (NEDO) performed a test. Two high-temperature geothermal wells Well-21 and WD-1a, which were drilled without lost circulation for the 8½" sections, were selected. The WD-1a well was drilled using the TDS-cooling method, and well-21 was drilled with the conventional technique when drilling high-temperature formations (Figures 27 and 28). As for the well-21 bit performance, tri-cone bit O-ring seals survived and average drilled hours of the three bits was 28 hours. The deepest depths where O-ring seals survived was 2105 m where the static formation temperature was 350˚C. Whereas, for the WD-1a well, the depth of the last bit for which O-ring seals still survived was 3451m; the bits were drilled for 31 hours where the static formation temperature was more than 450˚C. The average drilling time of the 5 bits without O-ring seal failures was 50 hours, where the static formation temperature was between 350 and 450˚C. Judging from the bit performances for the two wells, bit life using TDS-cooling method would be three to six times greater compared to the conventional cooling method if the same formation temperature and depths were drilled.

Economic evaluation of using TDS-cooling was made based on the field data when these two extreme high-temperature wells were drilled. Two examples are considered that compare the drilling of two 1000 m sections of an 8½" hole. Example 1: Drilling 8½" section of the well from 2500 to 3500 m. Example 2: Drilling 8½" section of the well from

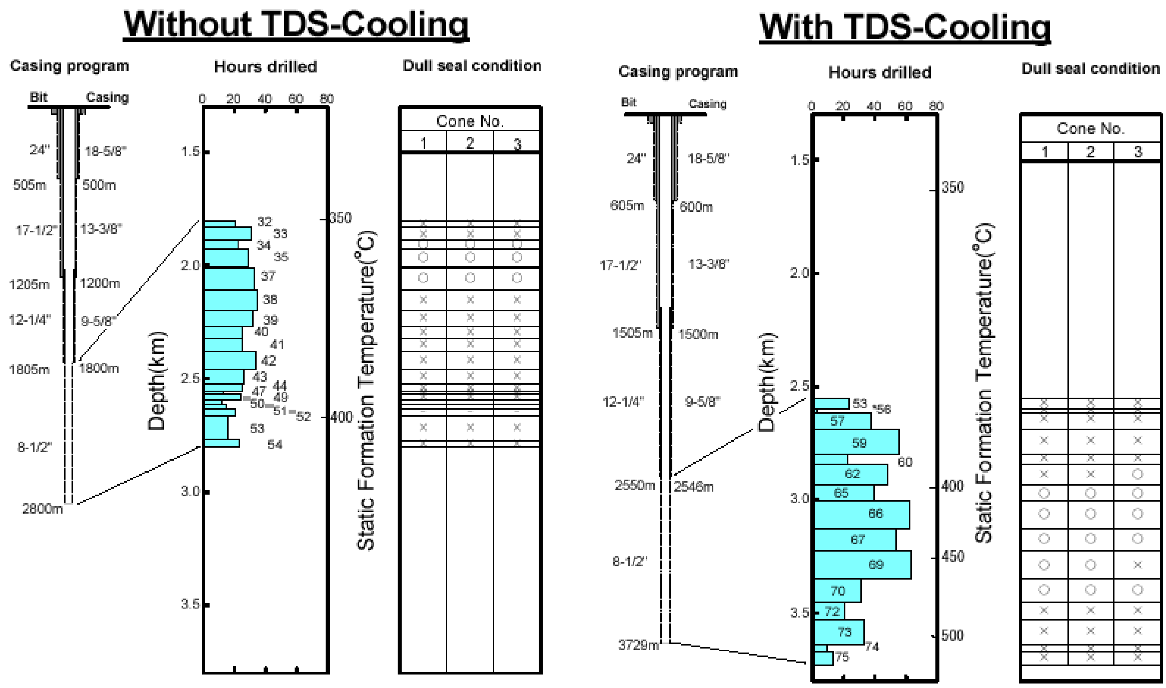

FIGURE 28: Bit performance and dull seal condition of 8½" bit used in well-21 and well WD-1A, Japan, with and without TDS cooling (Saito and Sakuma, 2000)

2000 to 3000 m. The cost factors, times and bit life for each example were based on actual data. Simulation results show that the TDS-cooling resulted in more economical drilling costs for both cases. The many other advantages of using TDS are described and indicate that it will be very economical to use TDS when drilling high-temperature wells (Satio and Sakuma, 2000).

3.8 Down-hole problems and prevention

Safe operations are of prime importance in geothermal well drilling, not only to protect the environment but also to insure against loss of lives and damage to property. Downhole accidents generally include blowouts, stuck pipe, drill string failure and bit problems. Off all the downhole problems, blowouts are the most dangerous and costly accidents and could be disastrous for a human being.

3.8.1 Well control

Typical blowouts in geothermal wells. There are many reports about blowouts in the petroleum industry costing millions of dollars every year. Although there are only a few cases reported in geothermal areas, it is important that all personnel dealing with it understand thoroughly what causes blowouts and how to avoid and control it.

Well KS-8 in Kilauea in Hawaii. In June 1991, a high-pressure/high-temperature well, KS-8, located in Hawaii kicked and unloaded at 1059 m. That well was estimated to have a possible bottom hole temperature of 343°C and a reservoir pressure approaching 160 bars. Immediate attempts to kill the well were unsuccessful, and the long process of well control was started. After 3 months of restoring the rig and equipment, pumping water to cool the well, snubbing out the drill string and replacing it with 7″ casing, pumping mud and cement to block the cross-flow, the final kill procedure was successfully performed, and well KS-8 was brought under control (Rickard et al., 1995).

Well NJ-11 in Nesjavellir, Iceland, is another case of an underground blowout. That well was drilled to 2265 m depth in 1985. Unexpectedly high temperatures and high pressures were met in that well. Controlling the well after drilling was exceptionally difficult. The pressure was deemed from the well's behaviour to have been well over 222 bars. The bottom hole temperature was at least 380°C, but could have been higher. Many attempts to seal off the loss zone at 1250m were unsuccessful, finally the well was partly filled up with sand.

The critical point of well control for the deep well. Well control equipment is the first line of protection against blowouts, but experienced operators and personnel dealing with drilling operation are more important. Personnel dealing with the drilling operations must be well trained and be aware of what problems a powerful geothermal resource can cause and what innovative procedures will be required to safely exploit those resources. Preventing the well from kicking is the first goal. Safety meetings and information meetings must be conducted before spuding the well and also at each stage of the project for all personnel. A good well design and a good cement job are also needed.

For a geothermal well, 4000-5000 m deep, the well control is much more important than before. When drilling a hole from 700 to 2300 m, several loss-of-circulation zones will probably be met and total circulation losses will occur at the upper reservoir at 1900-2200 m depth. In this section, there may also be some fractures connected to the deep supercritical zone, as was the case in well KS-8 in Hawaii and well NJ-11 at Nesjavellir. To prevent underground blowouts, a good practice is to block all the weak zones by cementing. Soundly casing this section off is also important. Leak off testing for the new formation below the casing shoe is necessary. The next section, from 2300 m to 3400 m has the same requirement as the section above. With increasing depth, temperature and pressure elevate and well control becomes even more important than before. Monitoring the temperatures and circulation loss every

15-20 minutes and blocking circulation loss zones immediately is required for safe drilling. After the 9⅝″ production casing is run and the cement job finished, check the BOP stack and pressure test again. Casing pressure testing and leak off testing for the new formation are also required. When drilling into the section below 3500 m, supercritical fluid will probably be met. The powerful geothermal water/steam may cause many problems. Requirements for well control are the same as mentioned above, and the driller must fill the well with water/mud and keep the over-balance of the well. Any mistake in operation will cause a huge loss!

3.8.2 Failure control of drill string components

Geothermal drilling is usually performed with the traditional rotary methods used in petroleum drilling, which produces a rotation of the whole drill string, from the surface to the bottom. In such a situation, all the drill string components are subject to variable stresses depending on the position occupied in the string. The main stress on the string is due to its own weight and increases from the bottom of the hole to the surface. Bending stresses are also present in directional wells or crooked holes (Massei and Bianchi, 1995).

In drilling operations, the main causes of drill string failures are cyclic bending and rotating bending stresses which can lead to failure of the components from fatigue in a matter of hours, especially when the well axis is particularly irregular, leading to increased tensile and bending stresses. The second cause is the corrosion by fluids encountered during drilling, and the third is an inadequate quality control system which fails to prevent defective components with potential crack initiations from being introduced into the well.

Geothermal drilling is, in most cases, done in dishomogeneous formations at a very low drilling rate, and in total or partial absence of circulation returns to the surface. The higher chemical aggressiveness of the fluids circulating in geothermal wells, the lower fluid level in the wells, which strongly limits the damping effect on vibrations, while higher well temperature, sometimes over 500°C, creates more extreme condition than during oil drilling. And deep geothermal well drilling is tough on drill string components. As a result, geothermal drilling requires drill string components which exceed the API standard. A good quality control system for the drill string is also required.

Inspections of drill string components play a fundamental role in reducing failures. Inspections of the drill string components includes two phases, inspections and tests during manufacturing and operations.
The reliability of a component is determined during the manufacturing phase. A component that has been designed and manufactured under quality conditions gives greater guarantees in terms of performance and service life. The manufacturers are required to carry out non-destructive inspections on the production line using not only the electromagnetic system, which mainly detects superficial external defects, but also continuous ultrasonic inspection, which reveals defects located in the "end area", in the metal thickness and on the internal surface. Specifications should guarantee the purchase of a quality product, suitable for use for geothermal fluids. The quality of the purchased components should always be kept as high as possible, even after use in the wells. But on-site inspections, before and after the drill string components are run into the well, are more important than the quality guarantee of the manufacturer. Any small mistake in handling during transportation may lead to defects in the drill string components and any small defects may lead to a fishing job in the well. All the drill string components need to be checked, such as size and thickness, shoulders and threads, using the electromagnetic system to detect superficial external defects, and continuous ultrasonic inspection before the drill string is run into the well, using the same methods to inspect the drill string components on every trip. Change the drill pipe position on every trip when the well is going deeper. Any defects made by pipe tongs or slips may also cause the failures of the pipes. Develope pipe management and a utilisation system and inspection record; form a data base to reconstruct the pipes history and conduct systematic drill string inspections depending on the working hours of the pipes; all these are parts of a quality control system.

3.8.3 The drill bit

With increasing well depth, more bit problems will occur. A TDS system is recommended to be used to cool down the bit while running into the hole, but the bottom hole temperature may still be too high and affect the bit life. According to temperature modelling mentioned in chapter 3.3.4, the bottom hole circulation temperature is still as high as 200°C or higher at 4000 m depth. It will exceed the temperature limitation of the sealed bearing of the bit. The formation becomes abrasive with increasing depth, so a new kind of bit with high temperature resistance needs to be developed for the job. The PDC or TSP bit may be a good choice for such deep well drilling.

3.8.4 Wellbore stability and drill mud

Conventional wells (less than 2500 m deep) drilled in Iceland suggest that the wellbore is very stable and few well bore collapse problems occur while drilling. Instead of using mud, only water is used for drilling. But with increasing well depth, well bore stability may become a problem. If there was a well bore collapse and a stuck pipe in a deep well, a huge sum of money could be spent for the fishing job! It may become necessary to use mud for deep drilling if there is a wellbore collapse problem. The conventional drill mud materials have a temperature limitation below 300°C; the maximum temperature limit is 350°C. So a new kind of drill mud material must be developed and a drill mud cooling system implemented for the high-temperature well.

4. CONCLUSIONS

The foreseeable need for deep drilling for exploitable hydrothermal fluids in Iceland during the 21st century calls for research on supercritical hydrous fluids. The high-temperature geothermal systems within the rift zones in Iceland provide several options for finding suitable targets for supercritical fluids. Tentatively, the active rift zone at Reykjanes, the landward extension of the Reykjanes Ridge, has been selected as a suitable target.

When drilling into supercritical conditions, many problems may occur due to severe conditions related to increasing well depth and rising temperatures and pressures, so a new advanced technology is needed. This study indicates that such a well can be cooled considerably while being drilled. But the casing and cement, well control, wellhead and downhole tools still need further study. The technical gain from deep drilling and research could have a global impact on geothermal utilization and is a challenging project worthy of international collaboration.

ACKNOWLEDGEMENTS

I would like to express my heartfelt gratitude to Dr. Ingvar Birgir Fridleifsson for giving me the opportunity to attend the UNU Geothermal Programme. I would like to express my gratitude to Mr. Sverrir Thórhallsson, my advisor, for his assistance, guidance and discussions during preparation of the report and also his generous hospitality. I am much obliged to Dr. Árni Ragnarsson, for his help and critical advice for this report. I wish to give thanks to Mr. Ómar Sigurdsson, Dr. Gudmundur Ómar Fridleifsson and Mr. Ásgrimur Gudmundsson for their willingness to help. And thanks to all the lecturers, and staff members at Orkustofnun for their comprehensive presentations in sharing their knowledge and experience.

Thanks go to Mr. Lúdvík S. Georgsson for all the care and generous help and advice during the whole training period. And, thanks to Mrs. Gudrún Bjarnadóttir for her wonderful care. My deep appreciation is due to my mama and my wife for their love and inspiration.

REFERENCES

API 1992: *Specification for casing and tubing (US customary units)*. API, specification 5CT (SPEC 5CT), 4th edition.

Bjarnason, J.Ö., 1985: *The computer program STEAM.* Orkustofnun, Reykjavík, report OS-85069/JHD-09 (in Icelandic), 129 pp.

Björnsson, S., Arnórsson, S., and Tómasson,T., 1972: Economic evaluation of Reykjanes thermal brine area, Iceland. *Am. Assoc.Petr. Bull., 56-12,* 2380-2391.

Chiba, M., Takasugi, S., Hachino, Y., and Muramatsu, S.,1988: Estimating of equilibrium formation temperature by curve fitting method. *J. Geothermal Research Soc. of Japan, November,* 383-386.

Fournier, R.O., 1983: Self-sealing and brecciation resulting from quartz deposition within hydrothermal system (abs.). *Proceedings of the 4th International Symposium on Water-Rock Interaction, Japan*, 137-140.

Fournier, R.O., 1985: The behaviour of silica in hydrothermal solutions. *Rev. Econ. Geology, 2,* 45-61.

Fournier, R.O., 1999: Hydrothermal processes related to movement of fluid from plastic into brittle rock in the magmatic-epithermal environment. *Econ. Geology, December*, 1193-1211.

Fridleifsson, G.Ó., and Albertsson A., 2000: Deep geothermal drilling on the Reykjanes ridge opportunity for international collaboration. *Proceedings of the World Geothermal Congress 2000, Kyushu-Tohoku, Japan*, 3701-3705.

Fujino, T., and Yamasaki, T., 1985: The use of fluid inclusion geothermometry as an indicator of reservoir temperature and thermal history in the Hatchobaru geothermal field, Japan. *Geoth. Res. Council, Transactions, 9,* 429-433.

Karlsson, Th., 1978: Casing design for high temperature geothermal wells. *Geoth. Res. Council, Transactions, 2,* 355-358.

Martin, J.C., Wegner, R.E., and Kelsey, F.J., 1976: One-dimensional convective and conditive geothermal heat flow. *Proceedings of the 2nd Workshop on Geothermal Reservoir Engineering, Stanford University, California*, 251-261.

Maruyama, K., Tsuru, E., Ogasawara, M., Inoue, Y., and Peters, E.J., 1990: An experimental study of casing performance under thermal cycling conditions. *SPE, Drilling Engineering, 1990,* 156-315.

Massei, S., and Bianchi, C., 1995: Failure control of drill string components: Nondestructive inspections. *Proceedings of the World Geothermal Congress 1995, Florence, Italy, 2,* 1427-1432.

Mondy, L.A., and Duda, L.E., 1984: *Advanced wellbore thermal simulator GEOTEMP2, user's manual.* Sandia, report SAND-84-0857, 147 pp.

New Zealand Standard, 1991: *Code of practice for deep geothermal wells*. Standards Association of New Zealand, Wellington, NZ, 93 pp.

Nicholson, R.W., 1984: Casing design for temperature regimes in geothermal wells. *Geoth. Resourc. Council Bulletin, May,* 23-26.

Pálmason, G., 1971: *Crustal structure of Iceland from explosion seismology.* Soc. Sci. Isl., 40, 187 pp.

Parasnic, D.S., 1971: Temperature extrapolation to infinite time in geothermal measurement. *Geophys. Prosp., 19*, 612-614.

Rickard, B., Livesay, B.J., Teplow, B., Winters, S., Evanoff, J., and Howard, W.T., 1995: Control of well KS-8 in the Kilauea lower east rift zone. *Proceeding of the World Geothermal Congress 1995, Florence, Italy, 2,* 1463-1466.

Saito, S., and Sakuma, S., 1997: Frontier geothermal drilling operations succeed at 500°C BHST. *Soc. Petrol. Eng./ International Association of Drilling Contractors (SPE/IADC 37625),* 445-458.

Saito, S., and Sakuma, S., 2000: Economics of increased bit life in geothermal wells by cooling with a top drive system. *Proceedings of the World Geothermal Congress 2000, Kyushu-Tohoku, Japan*, 2405-2409.

Schmidt, E., 1979: *Properties of water and steam in SI-Units* (2nd revised edition). Springer-Verlag, Berlin. 205 pp.

Snyder, R.E., 1979: Casing failure in geothermal wells. *Geoth. Resourc. Council, Transactions, 3*, 667-670

Stefánsson, V., and Björnsson, S., 1982: Physical aspects of hydrothermal systems. *Continental and Oceanic Rifts, Geodynamics Series, 8,* 123-145

Steingrímsson, B., Gudmundsson, Á., Franzson, H., and Gunnlaugsson, E., 1990: Evidence of a supercritical fluid at depth in the Nesjavellir field. *Proceedings of the 15th Workshop on Geothermal Reservoir Engineering, Stanford University, California*, 81-88.

The American National Standards, 1973: *ANSI B-31.1, power piping and ANSI B31-1.3, petroleum refiner piping.* American National Standards.

Thermie Project GE-0060/96, 1998*: Demonstration of improved energy extraction from a fractured geothermal reservoir.* Orkustofnun, Reykjavík report OS-98050, 42 pp.

Thomas, P.D., 1967: *High temperature tensile properties of casing and tubing.* Presented at the API Division of Production 1967 Midyear Standardization Conference, San Francisco, Ca.

VDI, 1963: *VDI Heat Atlas (in German*). VDI - Verlag GmbH, Dusseldorf.

Wong, H.Y., 1977: *Heat transfer for engineers.* Longman, London and New York, 236 pp.